Journal of the Indian Institute of Science
A Multidisciplinary Reviews Journal
ISSN: 0970-4140 Coden-JIISAD

REVIEWS

Recent NMR Methodological Developments for Chiral Analysis in Isotropic Solutions

*Sachin Rama Chaudhari and N. Suryaprakash**

Abstract | Chiral auxiliaries are used for NMR spectroscopic study of enantiomers. Often the presence of impurities, severe overlap of peaks, excessive line broadening and complex multiplicity pattern restricts the chiral analysis using 1D ^{1}H NMR spectrum. There are few approaches to resolve the overlapped peaks. One approach is to use suitable chiral auxiliary, which induces large chemical shift difference between the discriminated peaks ($\Delta\delta^{R,S}$) and minimize the overlap. Another direction of approach is to design appropriate NMR experiments to circumvent some of these problems, viz. enhancing spectral resolution, unravelling the superimposed spectra of enantiomers, and reduction of spectral complexity. Large number of NMR techniques, such as two dimensional selective F_1 decoupling, RES-TOCSY, multiple quantum detection, frequency selective homodecoupling, band selective homodecoupling, broadband homodecoupling, etc. have been reported for such a purpose. Many of these techniques have aided in chiral analysis for molecules of diverse functionality in the presence of chiral auxiliaries. The present review summarizes the recently reported NMR experimental methodologies, with a special emphasis on the work carried out in authors' laboratory.

1 Introduction to Chirality

The chiral objects are those that cannot be changed into their mirror images either by rotation or translational operation. As a result, handedness can be defined for chiral objects. In nature, right from the beginning of the evolutionary system, there is a great influence of chirality. Numerous examples of macroscopic chiral objects are available in nature. The classic example of macroscopic chiral objects is the human left and right hands. In fact the name chirality originates from the Greek word $\chi\varepsilon\acute{\imath}\rho$, meaning hand. The chirality is not restricted only to macroscopic objects and this concept also exists at the molecular level and has great significance.

1.1 *Molecular chirality*

The chemical compounds possessing identical molecular formula but different chemical structures are called isomers.[1–4] Isomers are further classified as structural or constitutional isomers and stereoisomers. Structural isomers have different connectivity of the constituting atoms, whereas stereoisomers have the same atomic connectivity but differ in their spatial arrangement. Enantiomers are a sub-class of stereoisomers where the sp^3 hybridized carbon atom attached to four different substituents results in non-superimposable mirror images. Molecules such as CCl_4, $CHCl_3$, whose mirror images can be superimposed are achiral, whereas molecules with non-superimposable mirror images are called chiral. The carbon atom with four different atoms or group of atoms is known as chiral carbon or stereogenic carbon. The important property of enantiomers is that they rotate the plane polarized light in opposite directions by an identical amount and the molecule is therefore

NMR Research Centre, Solid State and Structural Chemistry Unit, Indian Institute of Science, Bangalore 560012, India.
**nsp@nrc.iisc.ernet.in*

optically active. Except for this optical rotation property, the enantiomers have identical physical properties, such as melting point, boiling point, solubility, etc. Enantiomers that rotate the plane polarized light to the right, i.e. clockwise, are called dextrorotatory (*d*) and given symbol (+); those that rotate to the left, anti-clockwise, are called as laevorotatory (*l*) and the corresponding symbol is (−). The absolute configurations of such molecules are represented by '*R*' and '*S*'. As far as carbohydrates or amino acids are concerned, the same is represented by 'L' and 'D', instead of *R* and *S*. The equal mixture of enantiomers (1:1) is called racemic and is optically inactive. In nature there is a preferential occurrence for carbohydrates and amino acids. The naturally occurring carbohydrates are always D type and the naturally occurring amino acids are always L type. Such molecules of single enantiomeric form are called homochiral. There is no correlation between the configuration and the sign of the rotation. This is a general method employed for designating the configuration of each stereogenic unit in a given molecule.[5–7]

1.2 *Molecules with more than one stereogenic centres*

A molecule possessing a single stereogenic centre will possess only two enantiomer forms. On the other hand, molecules having two or three stereogenic centres give rise to four or eight stereoisomers respectively. As a general rule, a molecule containing *n* stereogenic centres can have a maximum of 2^n possible stereoisomers.

For clarity of the discussion, consider the tartaric acid molecule as an example. The chemical structure of tartaric acid given in Fig. 1 has two stereogenic carbons, numbered 2 and 3, and thus gives rise to a total of four stereoisomers. The configuration of four possible stereoisomers respectively for carbons 2 and 3 are, (*R, R*), (*S, S*), (*R, S*) and (*S, R*). The stereoisomers numbered 3 and 4 with configuration (*R, R*) and (*S, S*) are enantiomers. The presence of plane of symmetry in another set of enantiomers with configuration (*R, S*) and (*S, R*) gives superimposable mirror images and hence pertain to a single achiral molecule 5 with configuration (*S, R*), known as *meso* stereoisomer and is optically inactive. In brief, the *meso* stereoisomer of tartaric acid is achiral and possesses two self-cancelling stereogenic forms. The other combination of stereoisomers 3 and 5, 4 and 5 with respective configurations (*R, R*) and (*S, R*), (*S, S*) and (*S, R*) are not enantiomeric pairs. These stereoisomers do not have non-superimposable mirror image relationship unlike in enantiomers, and are referred to as diastereomers.

Unlike enantiomers, diastereomers have different physical properties such as boiling point, density, etc. These differences in the properties between diastereomers can be exploited to characterize and separate the mixture of enantiomers. The conversion of enantiomers to diastereomers is achieved by reacting the racemic mixture with an enantiopure reagent.

The chiral molecules with tetracoordinated atoms like N^+ (as in quaternary ammonium salts), Si, Ge, Sn, P, etc. bonded to four different substitutents are also known. There are certain class of molecules which are chiral, but do not possess any stereogenic centres. Nevertheless, in all these cases the basic condition for chirality is that the molecule and its mirror image should not be superimposable.[8,9]

1.3 *Importance of enantiomers*

The stereochemistry often determines important properties such as the chemical, physical, biological and pharmaceutical aspects of the compounds. Chiral compounds play a dominant role in the pharmaceutical industry and in the asymmetric synthesis.[10–12] More than half of the drugs in the pharmaceutical market are chiral. In most of the available drugs, only one enantiomer of the drug is effective against a particular disease, while its counterpart might be inactive, less active, nullify

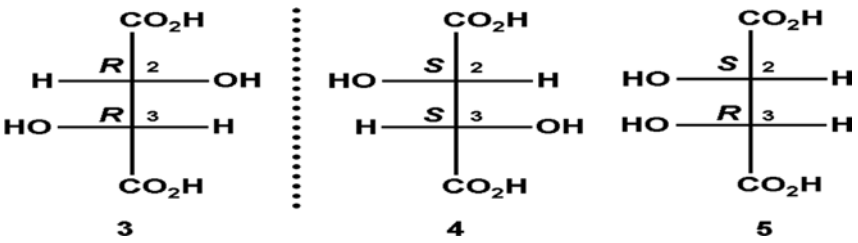

Figure 1: Stereoisomers of tartaric acid. Together structures 3 and 4 form enantiomers. Structure 5 is a meso compound. The structures 3 and 5, and 4 and 5 constitute diastereomers. The numbers 2 and 3 are associated with the stereogenic carbon atoms.

the effect or even be toxic. For example, the drug thalidomide was administered as the racemic mixture for the treatment of morning sickness associated with pregnancy. Subsequently it was found that only the (*R*) isomer was an effective sedative, whereas the (*S*) isomer caused severe deformities in babies. Therefore, assessment of the enantiomeric purity of the drugs has profound significance both in pharmaceutical industry and in asymmetric synthesis. There are various methods available for the separation of enantiomers, determination of *ee* (enantiomeric excess) and the assignment of absolute configuration.[13–19] Differentiation of enantiomers by NMR dates back to 1950's when Cram and his co-workers observed the non-equivalence of chemical shifts in diastereomers in 1959.[20] Ever since the work of Cram and co-workers, NMR spectroscopy has been proved to be a powerful technique, for testing the enantiopurity, measurement of *ee* and the determination of absolute configuration.[12,18,21,22]

2 NMR Spectroscopy and Chiral Analysis

NMR spectroscopy fails to distinguish enantiomers in the conventional achiral solvents, because of identical magnetic environment. It can easily be understood by Newman projections. As an example consider the molecule 2-bromo-1-chloropropanol, which has two chiral centres. The number of possible stereoisomers is 4 ($2^n = 4$, where n-is number of chiral centres) and all stereoisomers and their Newmann projections are shown in Fig. 2.

From the figure it is clear that 'a' and 'b' are non-superimposable mirror images of each other and form enantiomers. The Newman projections indicate that magnetic environment around each proton in the conformers 'a' and 'b' are identical. As a consequence NMR spectroscopy fails to distinguish the enantiomers. It is also true for the mirror images 'c' and 'd'. On the other hand, 'a' and 'c' are not mirror images of each other, and form diastereomers. The magnetic environments around protons in both 'a' and 'c' are different from each other; thus NMR can distinguish diastereomers. Similarly 'b' and 'c' form diastereomers and are distinguishable by NMR. Therefore, for the utility of NMR for chiral analysis, the basic requirement is that enantiomers are to be converted to diastereomers.[21,23] There are two major approaches to achieve this goal. The first one, called the classical approach, is widely employed. The classical approach is convenient and straightforward in many aspects, such as sample preparation and the use of simple one dimensional NMR experiments. In this approach, the conversion of enantiomers to diastereomers is carried

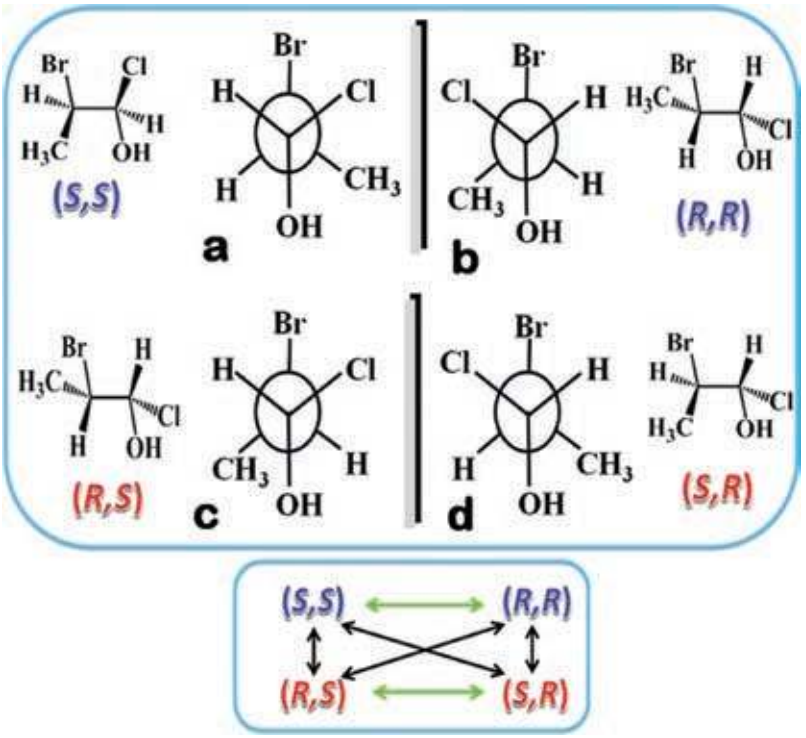

Figure 2: The representation of possible stereo isomers and their Newmann projections of 2-bromo-1-chloropropanol.

out by using any one of the chiral auxiliaries, viz., Chiral Derivatizing Agents (CDAs), Chiral Solvating Agents (CSAs) and Chiral Lanthanide Shift Reagent (CLSRs). The converted diastereomers permits the enantiodiscrimination and the precise measurement of *ee*. One of the requirements of classical approach is that the chiral solute (analyte) must contain certain functional groups, such as –COOH, $–NH_2$, –OH, etc., in order to convert them to diastereomers utilizing the derivatization protocol or non-covalent interactions. A general protocol utilized in such an approach is given in Fig. 3.

Another method involves the imposition of weak ordering to the chiral solutes by embedding them in a chiral aligning medium. Several aligning media have been reported for stereochemical applications, such as poly-γ-benzyl-L-glutamate, collagen gels, gelatines, cross linked poly(acrylonitrile), polysaccharide gels, fragmented DNA, etc.[24–31] Aligning the chiral molecules by embedding them in the weak chiral liquid crystalline matrix, whose order parameter is usually very low and is of the order of 10^{-3} or 10^{-4}, yields accessibility to more number of order sensitive NMR parameters, such as dipolar couplings, chemical shift anisotropies, and for nuclei with spin greater than ½ the quadrupolar couplings. Consequent to such interactions, many a times the NMR spectrum becomes too complex for straightforward analysis, and demands the use of higher dimensional NMR techniques, such as 2D or 3D experiments. Nevertheless, the natural Abundant ^2H NMR (NADNMR) is extensively used and voluminous amount of information is available in the literature on the use of NADNMR.[32–34]

2.1 *Advantages and limitations of different chiral auxiliaries*

Chiral Derivatizing Agent forms a covalent bond with the substrate moiety by a chemical modification.[35] The CDA produces chemical shift difference $(\Delta\delta)^{R,S}$ between diastereomers of *R* and *S* of chiral substrate that is very useful for testing the enantiopurity, measurement of *ee*, and also aids in the assignment of absolute configuration of enantiomers. The CDAs are specific to molecules containing particular functional groups. There are certain criteria required for choosing the CDAs, viz.; a) Substrate must contain some functional groups like –OH, –COOH, $–NH_2$, etc. in order to make esters, amide derivatives, etc.; b) Free from kinetic resolution (kinetic resolution refers to the condition where one isomer reacts faster than other isomer, giving rise to unequal intensity for diastereomeric peaks in the NMR spectrum; this gives errors in the measurement of *ee*); c) No racemization should occur during derivatization (racemization refers to the conversion of one isomer into another one); d) Diastereomers should have simple and well defined conformation in order to produce different magnetic

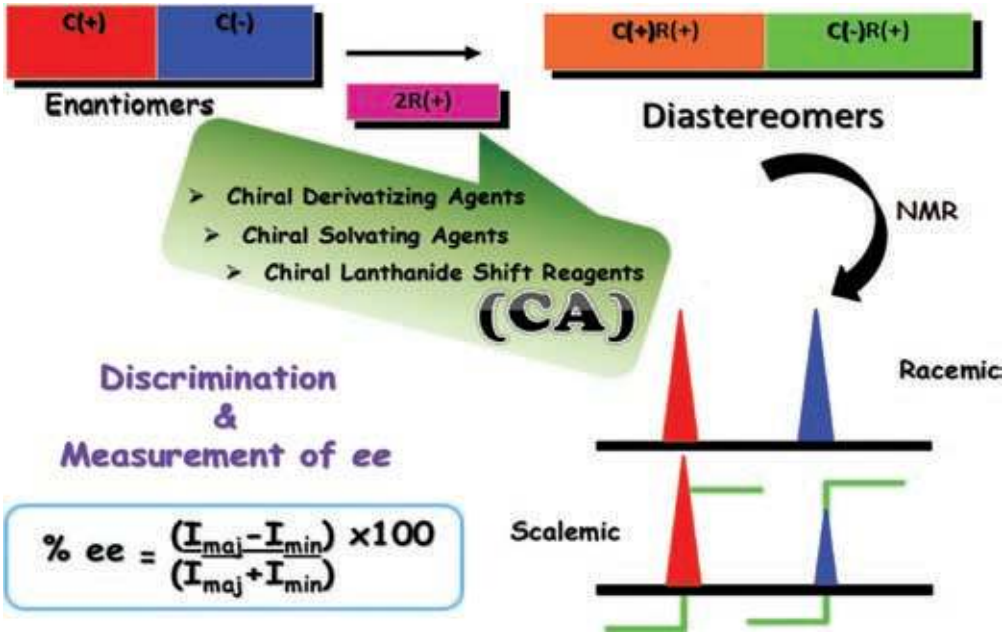

Figure 3: The graphical illustration of the general protocol utilized for discrimination of enantiomers using one of the chiral auxiliaries. The formula to measure the enantiomeric excess from the integral areas of the discriminated peaks is also given.

environments. The biggest advantage of the use of CDA is the larger $(\Delta\delta)^{R,S}$ between the discriminated peaks.

When chiral solvating agents are utilized the formation of diastereoisomers involves non-covalent interactions,[36] such as dipole-dipole, ion-pairing, -, hydrogen bonding, etc.[37,38] This is a simple mix and shake approach, as it involves only non-covalent interactions. Since non-covalent interactions are responsible for diastereomeric interactions, the $(\Delta\delta)^{R,S}$ depends strongly on physical parameters, such as concentration of CSA, temperature and the solvent employed.[39] At higher concentrations of CSA and lower temperatures the discrimination $(\Delta\delta)^{R,S}$ gets enhanced.[40] The commonly used CSAs are acids, amines, alcohols, sulphoxides, or cyclic compounds like cyclodextrins, crown ethers or cyclic peptides. One of the limitations of CSA is that $(\Delta\delta)^{R,S}$ obtained is relatively less compared to the use of CDA. The use of lanthanide shift reagent is a very old and well known concept in NMR. It can induce chemical shift changes of the substrate due to the influence of magnetic moment of an unpaired electron. If the ligand in the lanthanide complex is chiral then it is possible to obtain diastereomeric complexes. A complex formed between a paramagnetic material and a substrate can be used to differentiate enantiomers. Paramagnetic nature of the CLSRs cause excessive broadening of NMR peaks of chiral substrates. Similar to the use of CSA, the enhancement in $(\Delta\delta)^{R,S}$ is observed with increased concentration of CLSRs, which also results in broadening of the spectrum. Also, faster relaxation limits its usage at higher magnetic field strengths.

While doing enantio-discrimination ^{1}H NMR detection is generally favoured. However, the range of chemical shift spread of protons is very small. Thus, more often the overlap of peaks in the 1D ^{1}H-NMR spectrum restricts the measurement of chemical shift differences $(\Delta\delta)^{R,S}$ between the enantiomeric/diastereomeric peaks, and subsequent measurement of *ee*. Better discrimination is achieved (i) when the chemical shift difference between the discriminated peaks is large; (ii) concentration of chiral auxiliary is higher when CSA or CLSR is employed, (iii) the spectrum is devoid of severe overlap of discriminated peaks; (iv) there is not enormous broadening of spectral lines in spite of paramagnetic character of the lanthanide shift reagent, and (v) free from unreacted substrates (impurities). When any of these requirements is not fulfilled, the NMR utility for chiral analysis is severely hampered. There are few approaches to resolve overlapped peaks. One approach is to use a suitable chiral auxiliary, which induces large $(\Delta\delta)^{R,S}$ between the discriminated peaks and minimizes the overlap. This procedure demands the exploration of new chiral auxiliaries that usually involves skilful multistep synthesis and purification, and such chiral auxiliaries may not be commercially accessible. This restricts its general utility. Another way of overcoming some of these problems is to detect other NMR active hetero nuclei, such as, ^{19}F, ^{13}C, ^{31}P, ^{77}Se, etc. to derive the advantage of large chemical shift dispersion.[41–47] However, this requires the appropriate chiral auxiliary containing the heteronuclei, which may not be commercially available, and their synthesis might involve multiple steps thereby restricting routine use. Further, the low sensitivity and/or absence of such nuclei in the chiral molecules to be investigated also restricts their routine utility.

2.2 *Novel chiral auxiliaries and NMR methodologies*

There is a pool of chiral auxiliaries available in the literature, each of which is specific to molecules containing the particular functional group.[21,23] Nevertheless, there is continuous research to discover new, simple and convenient derivatizing and/or solvating agents to achieve discrimination of molecules possessing diverse functional groups. Our group has recently introduced several new protocols for enantiodiscrimination of chiral amines, hydroxy acids, carboxylic acids, diacids, amino acids, etc. The developed protocols serve as either solvating agents or derivatizing agents. Some of these protocols also yielded the stereospecific configuration of the molecules. As discussed earlier, at times the discrimination of enantiomers is hindered due to either very small chemical shift differences between the discriminated peaks or severe overlap of transitions from other chemically non-equivalent protons. Thus two pronged approach is adopted in this area of research. One is to introduce new chiral auxiliaries to achieve good chemical shift separation, and the other is to develop novel one and two dimensional NMR techniques to address the problems of spectral overlap and poor discrimination. The present review gives an account of recent developments in this direction, with a special emphasis on the results obtained by authors' group. Since this invited review is for the special issue on NMR spectroscopy and imaging, major impetus is given to NMR methodologies developed. Further, we would like to confess that this is not exhaustive and we have not been able to discuss the enormous and most important contributions made by different groups in this area of research.

3 NMR Methodological Developments

High sensitivity, high natural abundance, and ubiquitous presence of protons in majority of chiral molecules render the use of ^{1}H NMR by default as a most favourable choice. The prior requirements for chiral analyses are the simplification of spectral complexity that one might encounter and the straightforward identification of peaks pertaining to two enantiomers facilitating the determination of excess of one form over the other. In spite of enormous developments in NMR experimental techniques the challenge of measurement of chiral composition continues to persist, and there is a growing need for the development of simple, efficient and convenient experiments. The major cause for multiplicity is the scalar interactions of each chemically distinct proton with its coupled partners. Thus, one of the smartest ways of removing the complexity is to collapse these multiplets into singlets, enabling the straightforward measurement of chemical shift differences between the discriminated peaks. In addition to reducing the spectral complexity, unravelling of the overlapped spectra of enantiomers has an added advantage. For such a purpose, appropriate two dimensional experiments that are either resolved type or correlated type, are designed. These experiments could either be spin selective or non-selective. In situations when the chemical shift differences between the discriminated peaks are very small, one can detect higher quantum transitions where the additive value of the differential chemical shifts might enable discrimination. Again this higher quantum detection can be either by selective and non-selective. Many such recent experimental developments have paved the way for chiral discrimination. A comprehensive discussion on each of these reported techniques is given.

3.1 *ω_1-decoupled COSY technique*

It has been demonstrated that COSY and its variants can be employed for chiral discrimination.[48–51] The disadvantage of COSY type experiments is the presence of chemical shift and coupling interactions both in F_1 and F_2 dimensions. The separation of two interactions is a well documented technique, where only couplings evolve in the indirect dimension, whereas the 45° tilt of the spectrum provides only chemical shifts in F_2 dimension.[52] Number of NMR experiments are available on enantiodiscrimination using residual dipolar couplings. Selective Refocusing (SERF) type of experiments refocuses the chemical shift in the F_1 dimension, and gives only coupling information.[53] The band selective small angle correlation experiment has also been proved to be an invaluable experiment for the measurement of small residual dipolar couplings from the severely overlapped spectra.[54] A two dimensional broadband decoupling version, which relies on the spatial encoding of the NMR sample, yields chemical shift differences between the discriminated peaks.[55] To achieve better discrimination, a selective F_1 decoupled experiment has been reported, where the retention of chemical shift information contributes to an additional parameter, provided there is a measurable chemical shift difference between the two enantiomers.[56] The utility of the selective F_1 decoupling technique has also been applied recently for scalar coupled spin systems.[57]

3.1.1 Pulse sequence for selective F_1 decoupled COSY experiment: The pulse sequence and the graphical illustration of the appearance of the typical spectral pattern in the F_1 decoupled spectrum are given in Fig. 4.[57]

The developed pulse sequence for selective F_1 decoupled COSY is given in Fig. 4. Initially a proton spin H_i of a molecule is excited by the application of a semi-selective $\pi/2$ pulse. Couplings between the spin H_i and other proton spins $H_{i\neq j}$ are refocused by the hard π pulse during the first evolution period t_1, whereas H_i spin experiences an overall '2π' rotation due to the application of a semi-selective π pulse on H_i. This allows coherences to evolve only due to its chemical shift. The free induction decay is then acquired during t_2. In the resulting 2D spectrum, there is a multiplet structure in the direct dimension due to $H_i - H_j$ interactions, but a singlet structure at each chemical shift in the indirect dimension. In short, the use of semi-selective pulses causes the multiplet to collapse into a singlet in the indirect dimension of a 2D spectrum. The utility of this technique for chiral discrimination has been demonstrated on several molecules, whose structures are given in Fig. 5.

3.2 *Enantiomeric discrimination in diverse situations*

Lanthanide shift reagents are paramagnetic compounds and have the ability to induce a paramagnetic shift on the neighbouring nuclear spins of molecular systems with which they interact. The intermolecular interactions being diastereomeric, each enantiomer experiences a unique chemical environment. The difference in the chemical shifts depends on the relative substrate/shift reagent concentration. In general, higher the concentration of

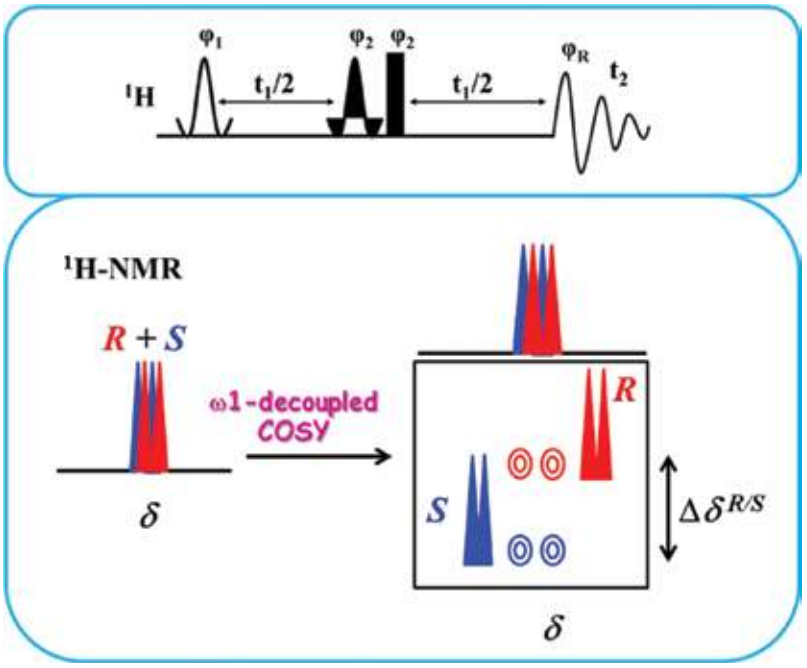

Figure 4: (Upper trace): Pulse sequence for the F_1 Decoupled COSY experiment. The phases of the pulses are $\varphi_1 = \varphi_R = x, -x$; $\varphi_2 = x$. (Lower trace): The schematic illustration of the appearance of ω_1-decoupled COSY spectrum depicting the unravelling of the spectrum of two enantiomers.

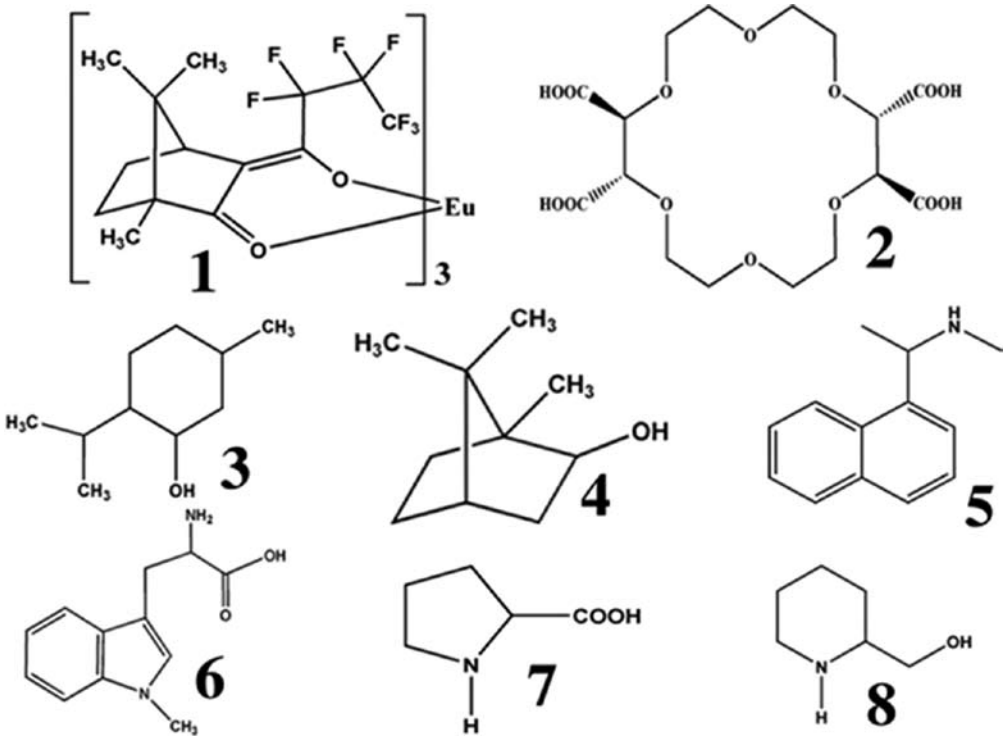

Figure 5: The chemical structures of chiral auxiliaries; europium(III)tris[3-(trifluoromethylhydroxymethylene)-(+)-camphorate (1), a chiral lanthanide shift reagent, and (18-crown-6)-2,3,11,12-tetracarboxylic acid (2), The chiral analytes are (±)-menthol (3), and (±)-isoborniol (4), (***R/S***)-N-methyl, 1-(1-naphthyl)ethyl-amine (5), (***R/S***)-1-methyltryptophanmethyl ester HCl (6), (D/L)-proline (7), and racemic 2-pipyridine methanol (8).

the shift reagent better is the chemical shift difference between the enantiomers. This is evident from Fig. 6, where for the sample of (±)-menthol in $CDCl_3$, at higher concentrations of europium(III) tris[3-(trifluoromethylhydroxymethylene)-(+)-camphorate, the Chiral Lanthanide Shift Reagent gave excessive line broadening due to paramagnetic relaxation, and resulted in poor resolution between the enantiomers. Therefore, the strategy of collapsing of multiplets into singlets using F_1 decoupled COSY technique has been employed to achieve enantiodifferentiation.

The ω_1-decoupled ^1H-^1H COSY spectra reported on the right side of Fig. 6, for chosen proton peaks, yielded a singlet for each enantiomer in the indirect dimension, which are marked with empty and filled rectangles to represent two enantiomers. The spectra are devoid of overlap and are ideal for the measurement of enantiomeric purity. The collapse of multiplets into well resolved singlets permitted unambiguous visualization of the enantiomers in the indirect dimension. This 2D experiment has also been applied on other molecules. The one and two dimensional F_1 decoupled COSY spectra of the molecule (±)-isoborniol in europium(III) tris[3-(trifluoromethylhydroxymethylene)-(+)-camphorate is given in Fig. 7. Clearly there is only a single broad peak at δ = 0.91 ppm in the 1D spectrum instead of two expected singlets, one for each enantiomer, causing a hindrance for enantiomeric discrimination. Though for the multiplets at δ = 2.09 and 4.02 ppm, partial resolution is visible and certain peaks are identifiable (in the F_2 cross section) for each enantiomer, the precise measurement of enantiomeric excess from such a spectrum is still a challenging task. On the other hand, the ω_1-decoupled 2D spectra selective on the multiplets centered at δ = 0.91 ppm reveals the total separation of overlapped enantiomeric peaks, which were otherwise impossible to resolve in the conventional 1D ^1H NMR spectra. Similar experiments at other selected proton chemical shifts also yielded two isolated singlets, marked as an open rectangle to represent one enantiomer and by the filled rectangle to designate the other enantiomer. The observation of two singlets in the indirect dimension in all the 2D spectra unambiguously

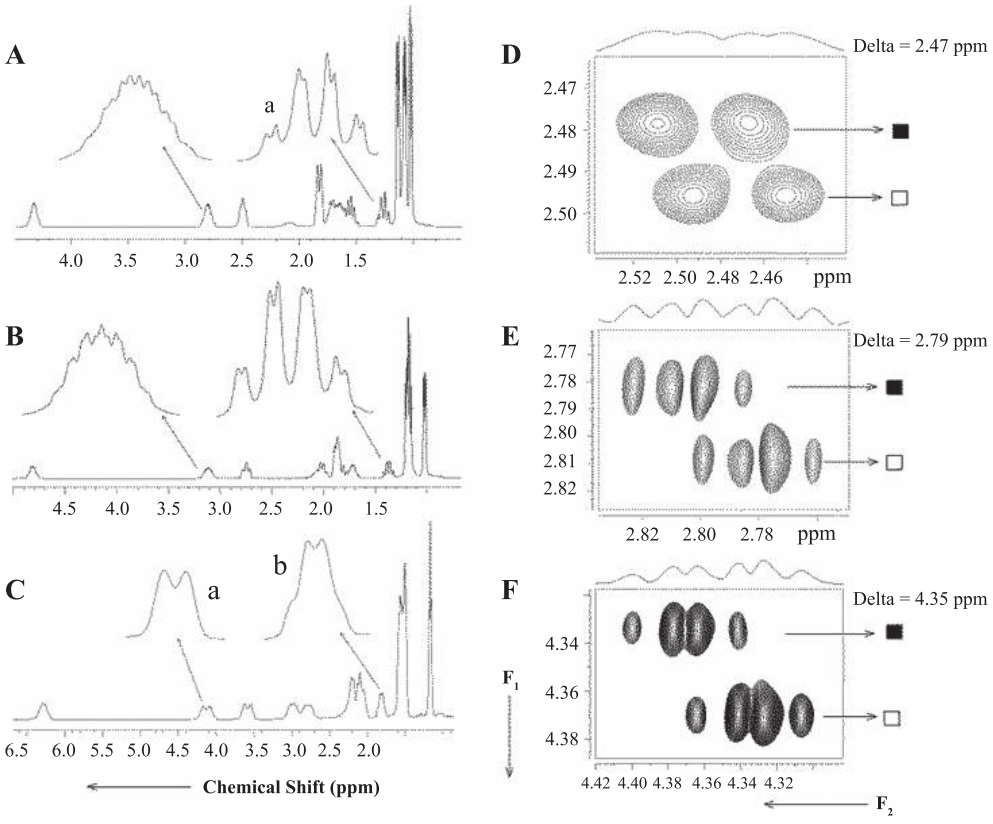

Figure 6: (A–C) are the respective ^1H NMR spectra of (±)-menthol in 13.9, 22.3 and 30.7 mM concentration of lanthanide shift reagent europium(III)tris[3-(trifluoromethylhydroxymethylene)-(+)-camphorate in $CDCl_3$. Chosen multiplets 'a' and 'b' are expanded; (D, E and F) are the selective 2D F_1-decoupled ^1H–^1H COSY spectra of in 13.9 mM of (±)-menthol for the overlapped multiplets resonating at δ= 2.47, 2.79 and 4.35 ppm, respectively.

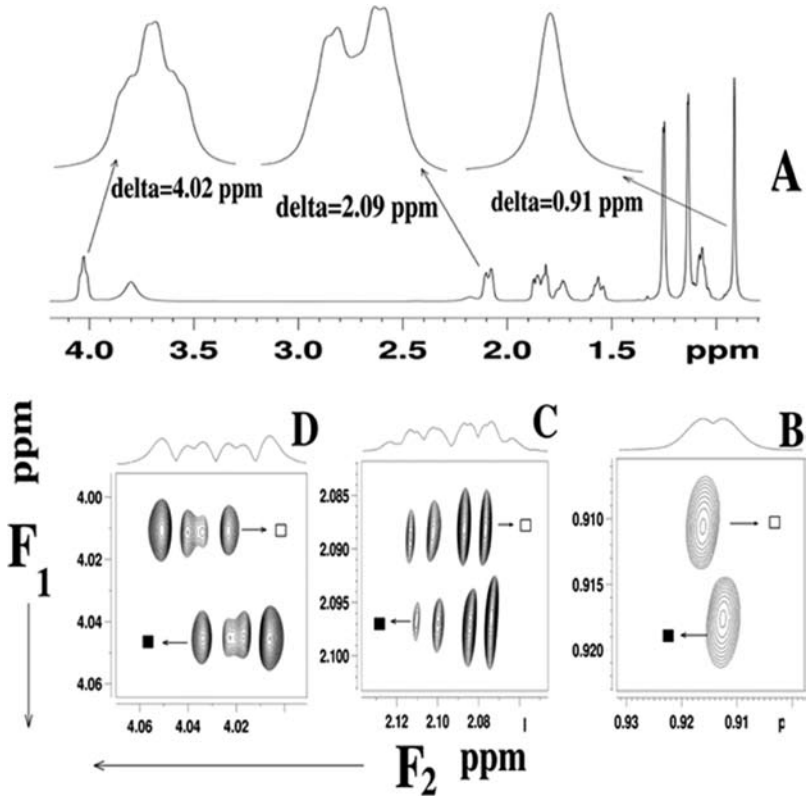

Figure 7: A) The 500 MHz ^{1}H NMR spectra of (±)-isoborniol in 13.7 mM concentration of europium(III)tris[3-(trifluoromethylhydroxymethylene)-(+)-camphorate in $CDCl_3$; (B)–(D) are the 2D ω_1-decoupled ^{1}H-^{1}H COSY spectra recorded for the overlapped multiplets centered at δ = 0.91, 2.09 and 4.02 ppm, respectively.

established the fact that a single selective experiment at any of the one overlapping multiplets would suffice to visualize enantiomers and also to determine the *ee*.

The NMR method of resolving the enantiomeric mixture employing the chiral solvating agent is very attractive for routine applications, as it does not require chemical modification through derivatizing agents. They are devoid of problems of recemization, undesirable chemical modifications or line broadening when the lanthanide shift reagents are used.[58] However, the degree of enantiodifferentiation is dependent on the concentration of CSA.[59] Especially, in case of amines, differences in chemical shifts between the enantiomers are smaller at low CSA concentration.[60] The use of ω_1 proton decoupled experiment overcomes such a limitation. Examples of these are reported for the measurement of *ee* for a primary amine, secondary amine and piperidine utilizing, (-)-(18-crown-6)-2, 3, 11, 12-tetracarboxylic acid as chiral solvating agent.

It is reported that for some secondary amines dissolved in chiral 18-crown-6, enantiomeric discrimination does not depend on the concentration of the latter beyond certain crown ether/substrate ratio.[60] As a specific example, the selected regions of ^{1}H NMR spectra of (*R/S*)-N-methyl 1-(1-naphthyl)ethylamine, marked 'a-e', obtained using chiral crown ether as an auxiliary is shown in Fig. 8. The multiplets centered at δ = 4.70 and 7.63 ppm at the CSA concentrations of 7.5, 10.2, 18.5, 26.4 and 33.6 mM respectively appear almost identical, showing very little degree of enantiodifferentiation. A close inspection of peaks at δ = 4.70 ppm reveals that although enantiomers are identifiable, measurement of accurate integral areas from these broad peaks and hence the determination of quantitative information is difficult. The 2D ω_1-decoupled ^{1}H-^{1}H COSY spectra recorded for multiplets centered at δ = 4.70 and 7.63 ppm dissolved in a CSA concentration of 7.5 mM yielded a distinct singlet for each enantiomer in the indirect dimension for both the spectra.

3.3 *F_1 decoupled experiment and* ee *measurement*

The F_1 decoupled experiment also permits the precise measurement of *ee*. This is demonstrated on a scalemic mixture of (*R/S*)-1-methyl tryptophan methyl ester HCl with an excess of 34.14% with *R*-enantiomer and the chiral 18-crown-6

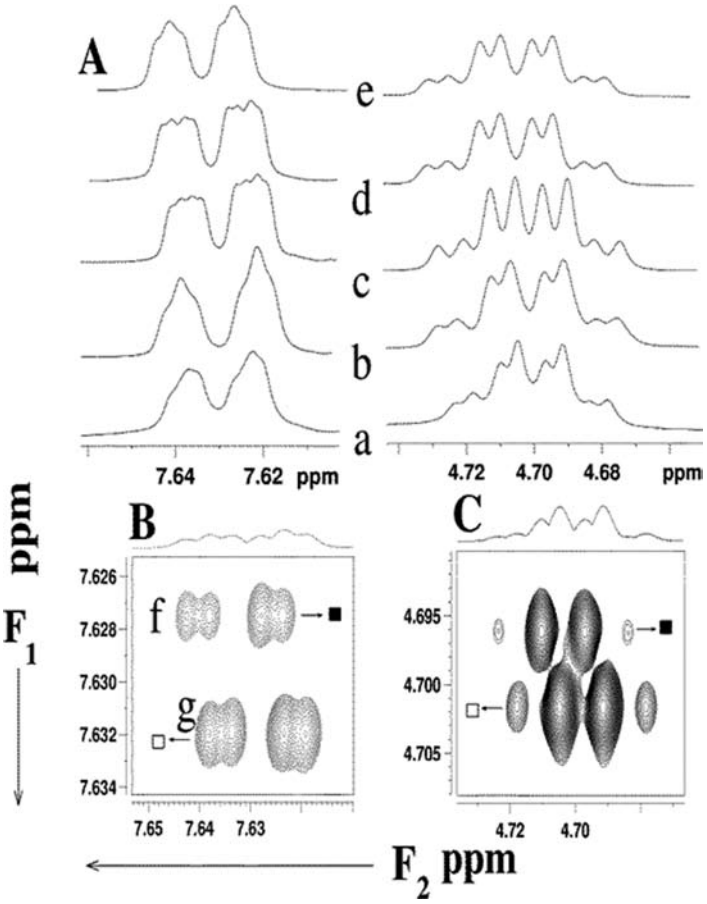

Figure 8: A) 'a–e' represent the regions of the ^{1}H NMR spectra of (***R/S***)-N-methyl 1-(1-naphthyl)ethylamine dissolved in 7.5, 10.2, 18.5, 26.4 and 33.6 mM concentrations of chiral 18-crown-6 ether, respectively; (B and C) are the 2D ω_1-decoupled ^{1}H–^{1}H COSY spectra carried out for the overlapped multiplets centered at δ = 7.63 and 4.70 ppm respectively.

ether concentration of 0.50 mM. The spectra are reported in Fig. 9. A part of the ^{1}H NMR spectra in the aromatic region exhibits little degree of enantiodiscrimination. Although the outer peaks of the spectra pertain to a single-enantiomer, the middle peaks are completely overlapped precluding the precise measurement of enantiomeric purity. On the other hand the ω_1-decoupled ^{1}H-^{1}H COSY experiment resulted in two singlets in the indirect dimensions that belong to the completely discriminated single-enantiomer spectra. An *ee* of 33.19% is obtained by volumes of the contours marked as 'a' and 'b'. Similar analyses for the selected protons of different molecules gave precise values of *ee* within experimental error to those expected from the gravimetric preparation.

4 RESolved TOCSY (RES-TOCSY) Technique

The previous method was developed to achieve discrimination through selective excitation of a particular spin. This aided the discrimination in many situations, viz., when the peaks are severely overlapped, or excessive broadened, etc. However, if one is interested in extracting the chemical shift difference for all other protons, multiple experiments are required to be carried out. In order to overcome this shortcoming, another two dimensional experiment cited as RES-TOCSY[61] has been developed, where in a single experiment it is possible to achieve discrimination at multiple proton sites.

4.1 *Spin dynamics of RES-TOCSY pulse sequence*

The designed pulse sequence and the graphical representation of a typical RES-TOCSY spectrum are reported in Fig. 10. The pulse sequence starts with a semi-selective $\pi/2$ pulse, which excites selective proton (H_i) in each enantiomer/diastereomer followed by t_1 evolution. During t_1 evolution the combined use of selective π pulse and a hard π pulse causes decoupling of H_i with the remaining protons, which allows the evolution of chemical shift of H_i only. Consequently, the separation

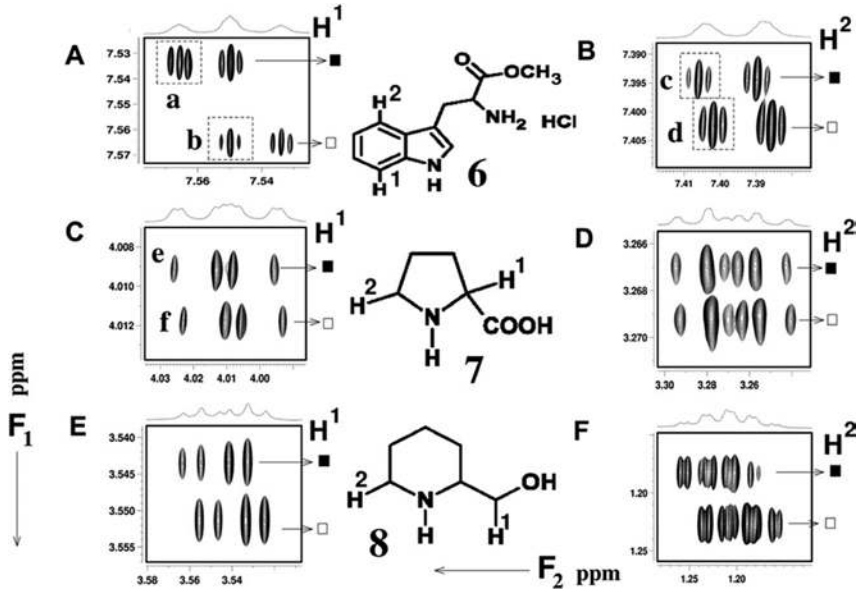

Figure 9: (A and B) are 2D ω_1-decoupled ^{1}H–^{1}H COSY spectra of (*R*/*S*)-1-methyl tryptophan methyl ester HCl in 0.50 mM of CSA for the multiplets centered at 7.54 and 7.39 ppm, respectively. (C and D) represent the 2D ω_1-decoupled ^{1}H–^{1}H COSY spectra of (D/L)-proline in 8.5 mM CSA centered at 4.0 and 3.26, respectively. (E and F) represent the 2D ω_1-decoupled ^{1}H–^{1}H COSY spectra of (*R*/*S*)-2-pipyridine methanol in 0.5 mM CSA for the overlapped multiplets centered at $\delta = 3.54$ and 1.20, respectively. In the all 2D spectra, projections shown in the direct dimension represent the normal ^{1}H spectra of enantiomers dissolved in the different concentrations of chiral 18-crown-6 ether. Peaks for one enantiomer are denoted by the filled rectangles and for other enantiomer by the open rectangles.

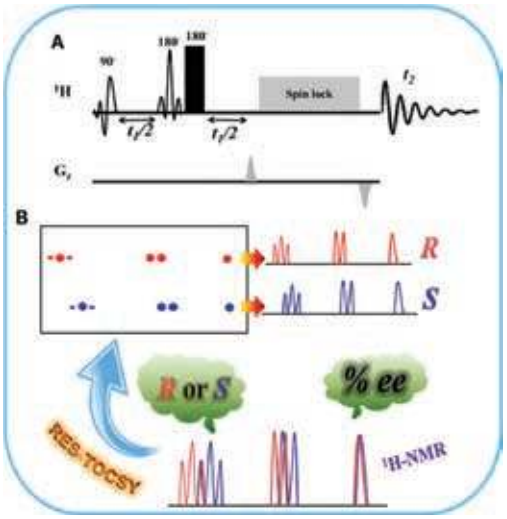

Figure 10: A) The RES-TOCSY pulse sequence, where the first and the second pulses are semi-selective $\pi/2$ and π pulses respectively. The thick rectangular pulse is hard pulse. The phases of semi-selective $\pi/2$ pulse, semi-selective pulse, hard pulse and receiver are respectively x, x, -x, x. Two z-gradients of equal magnitude and opposite signs are used for coherence selection. The spectrum is recorded in magnitude mode. B) Schematic representation of the RES-TOCSY spectrum, where the two overlapped spectra of enantiomers are completely unraveled.

of enantiomers/diastereomers peaks $(\Delta\delta)_i^{R,S}$ of H_i occurs in the indirect dimension. During isotropic mixing the separated protons magnetization is transferred to all other coupled protons of respective enantiomer/diastereomer, resulting in the evolution of both couplings and chemical shifts in the direct dimension. Therefore, only two traces of peaks appear in the indirect dimension, one for each enantiomer/diastereomer, the separation of which pertains to $\Delta\delta_i^{R,S}$ of H_i. In other words, although the $\Delta\delta^{R,S}$ of many discriminated peaks vary over a wide range in direct dimension, in the indirect dimension the separations of all the discriminated peaks are scaled to $(\Delta\delta)_i^{R,S}$ of H_i. This highlights the biggest benefit of RES-TOCSY experiment, since the peaks with small chemical shift separation (or completely overlapped) can also be resolved by judicious choice of excitation of peaks with larger $(\Delta\delta)^{R,S}$. The maximum scaling pertains to the maximum separation between the peaks, provided the peak can be selectively excited. This puts the limit on the scaling.

The RES-TOCSY experiment finds utility in the enantiodiscrimination on various chiral auxiliary-substrate systems, such as chiral derivatizing agent, chiral solvating agent and Chiral Lanthanide Shift Reagent, where the peaks are either overlapped and/or broadened due to diverse

reasons. In addition, the methods also permit the accurate measurement of *ee*.

4.2 *Resolution of enantiomeric peaks in the presence of unreacted species*

Chiral Derivatizing Agents (CDAs) are more often used for assignment of absolute configuration based on chemical shift values of diastereomers.[21,23,62–64] Initially the enantiomers are converted to diastereomers by derivatization process, which involves chemical reaction between CDA and substrate in the presence of a catalyst, under standard reaction conditions in a suitable solvent. The reaction mixture needs to be purified before it is subjected to NMR analysis, which is more time consuming and tedious process. The advantage of RES-TOCSY experiment in this situation is demonstrated on an example of iminoboronate ester of secondary butyl amine. The discrimination is achieved by stirring ternary mixture of butyl amine, *R*-BINOL and 2-formylphenylboronic acid in solvent $CDCl_3$ for 5 minutes. This procedure is based on the reported three component protocols.[65–67] The 1D ^{1}H spectrum of this iminoboronate ester, shown in Fig. 11 (upper trace), exhibits severe overlap around 1.7 ppm, because of multiplicity pattern and the presence of unreacted species (impurity peaks), which hampers the peak assignment. On the other hand, the 2D RES-TOCSY spectrum, given in Fig. 11 (lower trace), resulted in complete unraveling of the spectrum for both the enantiomers facilitating the easy analysis. The advantage of RES-TOCSY experiment becomes evident on closer inspection of peaks in the 1D spectrum, resonating at 1.7 ppm, where the discriminated peaks sitting on a broad hump have been unambiguously extracted. It is also evident that the peaks marked as * arising from the unreacted species (impurities) are completely suppressed.

4.3 *Resolving the broadened and overlapped spectrum*

Chiral analysis using Chiral Solvating Agents (CSAs) is easy as they involve non-covalent interactions.[63,64] Often, line broadening, especially at higher concentrations of CSA, in addition to multiplicity pattern, masks the differentiated enantiomeric peaks. Such problems are circumvented by the RES-TOCSY experiment as demonstrated on the molecule 1-aminoindane with BINOL as CSA in the solvent $CDCl_3$.[68,69] The 1D ^{1}H NMR spectrum shown in Fig. 12 (upper trace), exhibits unresolved differentiated enantiomeric peaks, severely hampering the chiral analyses. On the other hand, the 2D RES-TOCSY spectrum reported in Fig. 12 (lower trace), exhibits the completely unravelled peaks for each enantiomer. On

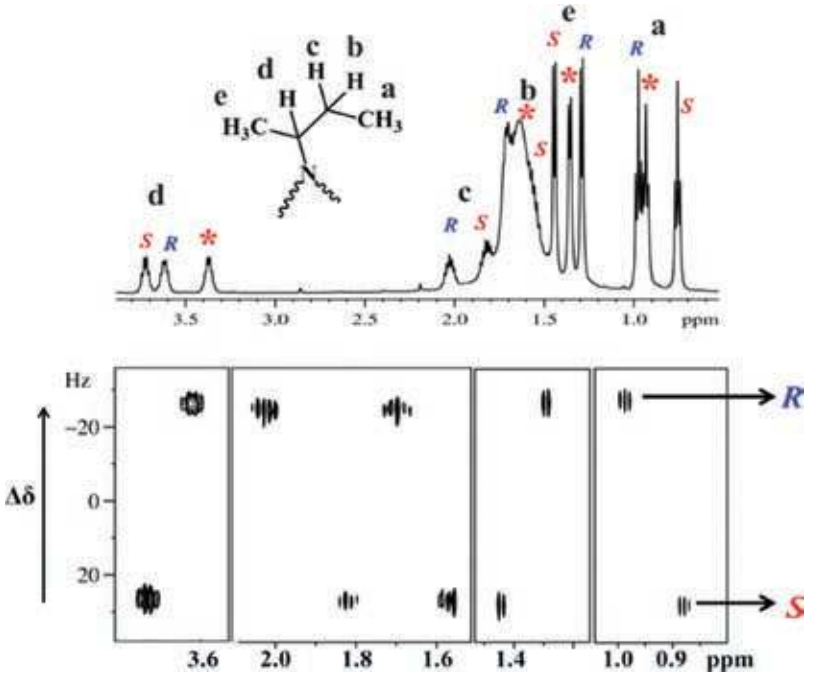

Figure 11: (Upper trace): 1D ^{1}H NMR spectrum of diastereomers of iminoboronate ester; (Bottom trace): the 2D ^{1}H RES-TOCSY spectrum obtained by selective excitation of proton labelled d in the chemical structure given.

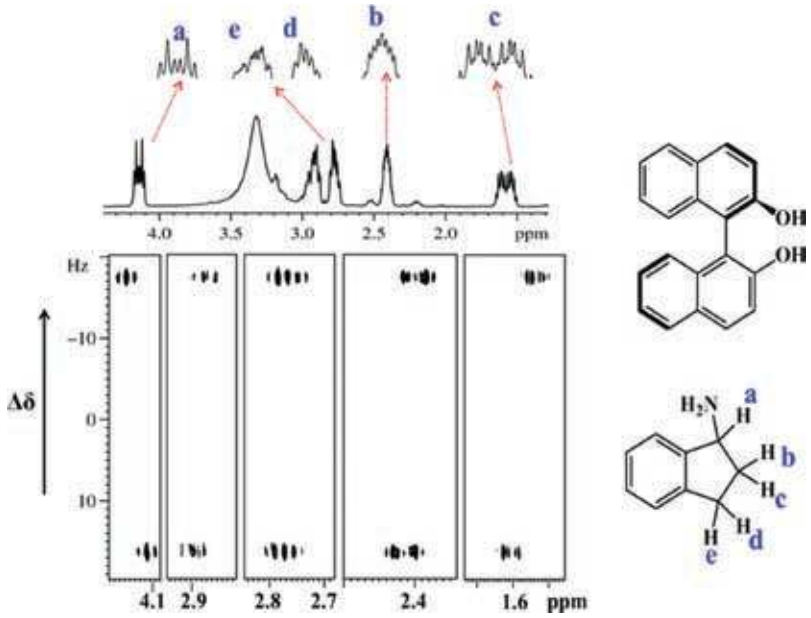

Figure 12: (Upper trace): 1D ^{1}H NMR spectrum of 1-aminoindane in the presence of chiral solvating agent *R*-BINOL; (Bottom trace): The 2D ^{1}H RES-TOCSY spectrum with selective excitation of proton labelled 'a'.

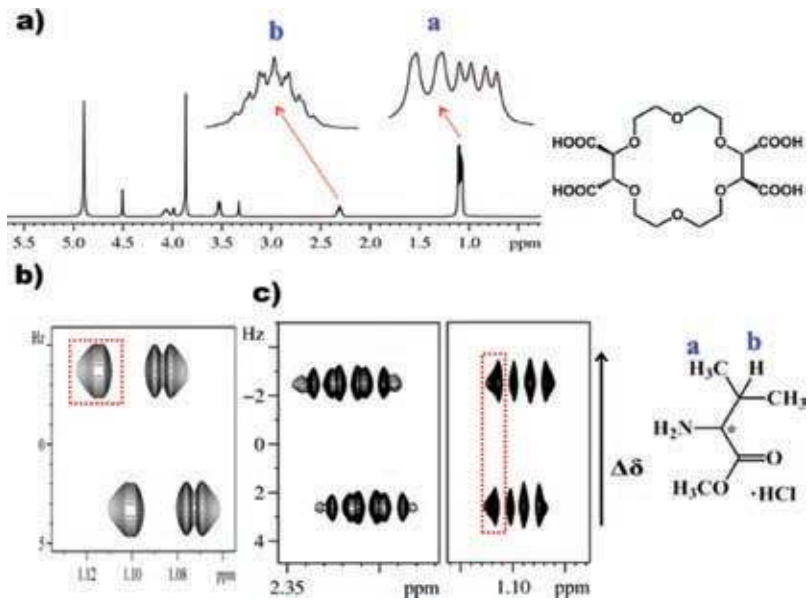

Figure 13: a) 1D ^{1}H NMR spectrum of valine methyl ester hydrochloride in the presence of chiral solvating agent (+)-(18-Crown-6)-2,3,11,12-tetracarboxylic acid; b) 2D ^{1}H *J*-resolved spectrum and c) 2D ^{1}H RES-TOCSY spectrum with selective excitation of proton 'b' recorded under identical conditions.

closer inspection of peaks marked 'b', it is clearly evident that the severely overlapped peaks in the 1D spectrum are unambiguously resolved in the RES-TOCSY experiment.

4.4 *RES-TOCSY vs J-resolved technique*

The RES-TOCSY technique is very useful in situations when the chemical shift separations are very small. For example, the peaks in the 1D ^{1}H NMR spectrum of valine methylester hydrochloride solvated by (+)-(18-Crown-6)-2,3,11,12-tetracarboxylic acid,[60,70] reported in Fig. 13a, shows severe overlap. The 2D-*J*-resolved (discussed in latter part of the review) and 2D RES-TOCSY spectra for the same sample are compared in Figs. 13b and 13c respectively. In the *J*-resolved

experiment the peak pertaining to chemical shift difference of nearly 4 Hz between the enantiomeric peaks are unresolved, which is shown in the direct dimension marked with dotted rectangle in Fig. 13b. On the other hand, the RES-TOCSY spectrum exhibits a clear separation in the indirect dimension (marked with dotted rectangle in Fig. 13c). This is a direct consequence of the scaling of $(\Delta\delta)^{R,S}$ of peaks 'a' to that of selectively excited peaks 'b' in the RES-TOCSY experiment. This scaling property of RES-TOCSY thus, has an excellent utility.

4.5 *When spectra are severely broadened by metal complex*

As discussed earlier, the 1D ^{1}H NMR spectroscopic differentiation of enantiomers using Chiral Lanthanide Shift Reagent is always hindered due to severe broadening of peaks, thereby hampering the analysis.[71,72] Furthermore, CLSR has a restricted utility for chiral discrimination, especially in high field spectrometers, as the lines get more broadened.[73,34] This is observed in the 1D ^{1}H NMR spectrum of exo-norborneol with CLSR (*R*)-Eu(tfc)$_3$ in the solvent $CDCl_3$ given in Fig. 14. The differentiated enantiomeric peaks are masked due to severe line broadening. On the other hand, the 2D RES-TOCSY spectrum for the same sample, reported in Fig. 14, displays differentiated peaks for each enantiomer, facilitating the analyses.

4.6 *RES-TOCSY and enantiomeric excess measurement*

The RES-TOCSY technique also permits the measurement of enantiomeric composition. This has been ascertained on the sample *R* and *S* alphamethylbenzylamine with BINOL as chiral solvating agent.[69,70] The *ee* has been determined by the RES-TOCSY experiment on samples of different scalemic ratios, and are compared with the gravimetrically prepared ones. The plot of experimental results versus the gravimetric data for different scalemic ratios reported in Fig. 15, exhibit an excellent correlation, confirming that this technique can be employed for precise measurement of *ee*.

5 Homonuclear Higher Quantum Technique

The previous two techniques developed for enantiodiscrimination pertain to detection of single quantum coherence by spin selective excitation. One may also encounter situations when the spectroscopic discrimination of enantiomers in the solution state and the measurement of enantiomeric composition is hindered due to either very small chemical shift differences between the discriminated peaks or severe overlap of transitions from other chemically non-equivalent protons. The selective excitation of a particular spin could then be difficult. One can then explore the possibility of selective excitation of group of

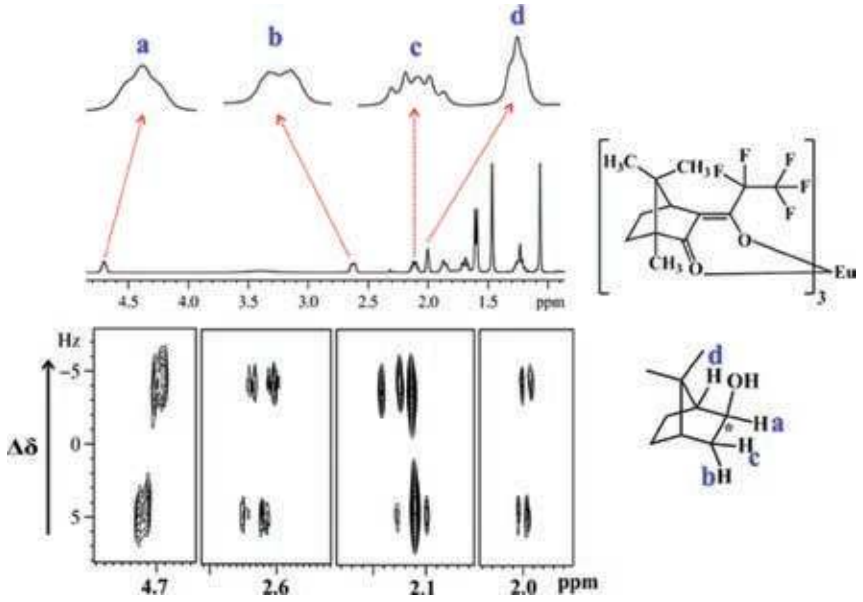

Figure 14: (Upper trace): 1D ^{1}H NMR spectrum of exo-norborneol in the presence of Chiral Lanthanide Shift Reagent (*R*)-Eu(tfc)$_3$ with expansions of selected regions identified by arrows; (Bottom trace): RES-TOCSY spectrum. The proton 'a' is selectively excited.

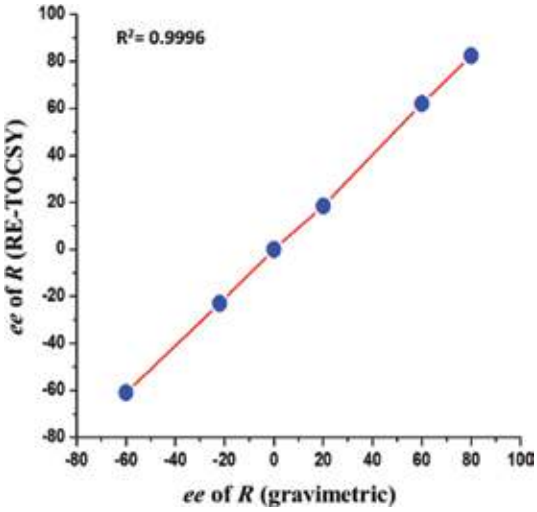

Figure 15: A plot of *ee* determined by RES-TOCSY experiment with those expected from the gravimetric composition.

scalar coupled spins and detection of maximum quantum coherence. This Multiple Quantum Technique (MQT) has an enormous advantage, especially when the conventional one dimensional ^{1}H NMR spectra fail to differentiate the enantiomers due to very small chemical shift difference between the discriminated peaks. This is due to the fact that the difference in the additive values of all the chemical shifts of a scalar coupled spin system, between the two enantiomers, is detected in the highest quantum. This might give substantial difference in the frequencies between the discriminated peaks permitting the discrimination. The utility of this unconventional MQT has also been employed for chiral analyses.[75] Before discussing utility of MQT for chiral analysis, a brief introduction to multiple quantum, the selective and non-selective detection of highest quantum coherence will be discussed.

5.1 *Multiple Quantum (MQ) NMR*

In conventional one dimensional NMR, the detected single quantum transition pertains to flipping of a spin between two energy states that differ in their total spin angular momentum (Δm_I) by ±1. On the other hand, in the detection of Multiple Quantum (MQ) transition, the change in the total spin quantum number between two energy states is anything other than ±1. Thus, the MQ coherence is a coherent superposition of energy states for which Δm_I is anything other than ±1.[76] The excitation and detection of any quantum including zero quantum falls under the category of MQ experiments. The spins that collectively undergo transitions between the two states are referred to as active spins, and all the remaining spins are said to be passive. The collection of all the active spins can be construed as a super spin and the remaining passive spins as spectator spins. The nature of the coherence depends both on the order of the detected quantum, the properties of active spins and their nature of interactions with the spectator spins. In simple terms the single quantum pertains to the situation where any one of the coupled spins is flipped in the presence of scalar fields of other spectator spins. Then the scalar fields from all the passive spins are available for interaction with this single spin. On the other hand, in multiple quantum transitions, many spins are allowed to flip at a time. It implies that as the size of the super spin increases, the number of spectator spins decrease, and consequently, the available scalar fields for interaction with active spins are reduced. Thus, higher quantum detection gives less number of transitions, and thereby the spectrum gets simplified.[76–78]

For N coupled spins, the highest quantum coherence is a situation where all the spins are active, and result in flipping at their respective chemical shift positions. The absence of any spectator spin results in a single transition for the highest quantum due to the absence of scalar couplings, and resonates at the sum of their chemical shifts.[76] N-1 quantum is a situation in which N-1 spins are active and a single left over spin is a spectator. The super spin is then split by the scalar field of a lone spectator spin resulting in a doublet centered at the sum of the chemical shift positions of the active spins. The doublet separation corresponds to the cumulative additive values of couplings between active spins and the passive spin. For N chemically non-equivalent spins there are N doublets in the N-1 quantum. The N-2 quantum coherence is a situation where N-2 spins flip at a time in the presence of the remaining two spins. This will have more number of transitions than N-1 quantum, but significantly less compared to SQ transitions. The number of transitions, and thereby the complexity of the spectrum, increases on going to lower quanta.[76–78] Furthermore, the precessional frequency of any higher quantum coherence is proportional to its order. Consequently, the field inhomogeneity also proportionally gets scaled up. Thus, the m^{th} quantum order is broadened by m times. However, the zero quantum coherence is insensitive to the field inhomogeneity. Voluminous information is available on the excitation and detection of higher quantum coherence.[79–85] The selection of particular higher quantum coherence is achieved by the application of pulse field gradients before and after the last

pulse, which converts MQ coherence to detectable SQ coherence. The gradient ratio defines the order of the quantum to be detected. This also implies that zero quantum selection is impossible by the application of gradients. The detection of zero quantum coherence is achieved by phase cycling.

5.2 *Non-selective excitation of multiple quantum*

All the MQ experiments employ a three pulse sequence. The multiple quantum orders are created during the evolution period and are subsequently converted into detectable single quantum coherence. Appropriate excitation and detection pulse sequences are employed based on the information to be derived. Excitation and detection sequences are designed by using either spin selective or non-selective pulses. The detailed discussion on MQ spectrum of different types of spin systems is available in the literature.[76] For example in a homonuclear three spin system of the type AMX there are three possible Double Quantum (DQ) excitations. One can non-selectively excite all the three possible DQ transitions, viz. AM double quantum (where A and M spins are active spins), AX double quantum (where A and X spins are active spins), and MX double quantum (where M and X spins are active spins). In the DQ-SQ correlation experiment the DQ dimension provides three sets of doublets at the sum of the chemical shifts of the two active spins. The separation of the doublets pertains to the sum of passive couplings, viz., $J_{AX} + J_{MX}$, $J_{AM} + J_{MX}$ and $J_{AM} + J_{AX}$ respectively for AM, AX and MX double quantum. Each component of these doublets corresponds to the $|\alpha>$ and $|\beta>$ states of the respective passive spin. The cross sections taken along the SQ dimension for any of the spin states of the passive spin, gives all the twelve transitions expected for an AMX spin system, whose intensities depend on the flip angle.[86] Thus, in a non selective detection each $|\alpha>$ and $|\beta>$ spin state of passive spins correlates to all the allowed transitions in the SQ dimension.

5.3 *Spin state selective detection of multiple quantum*

In the example of an AMX spin system discussed in the preceeding section, instead of non-selective excitation, if a pulse is applied selectively on any two spins and no pulse is applied on the third spin, then the states of the passive spin remain unperturbed both in DQ and SQ dimensions. This is the spin selective excitation in a homonuclear spin system. It may be emphasized that in the selective excitation the spins must be weakly coupled. In the case of heteronuclear spins the large chemical shift difference renders the heteronuclear spins weakly coupled. The non-selective excitation of homonuclear highest quantum coherence of heteronuclear spin systems retains the spin states of heteronucleus undisturbed. This is analogous to spin state selective excitation of homonuclear spins. Spin State selective techniques are extensively discussed in the literature.[87–108] In both the situations the passive spin(s) provide spin state selection. Then the spin states of the passive spins in the DQ dimension encodes the spin states involved in the SQ transitions that arise only due to coupling among active spins, and result in the selective detection of SQ transitions. The cross-section taken along SQ dimension for any one of the passive spin states has less number of transitions compared to the normal SQ spectrum, but suffice to determine the chemical shifts of active spins and the couplings among them. Thus, in the selective AM DQ excitation of AMX spin system, the cross section taken along SQ dimension for each spin state of passive X spin provides only four transitions instead of eight. Therefore, the spin state selection has a power of reducing the spectral complexity. The interesting feature of the technique is that it also achieves, in homonuclear spin systems, separation of passive couplings and active couplings in the MQ and SQ dimensions respectively. In heteronuclear spin systems, it achieves separation of homo and heteronuclear couplings, respectively, in direct and indirect dimensions.[87–109]

5.4 *Highest quantum spectra of scalar coupled chiral molecules*

The applications of MQ methodology for the simplified analyses of the complex spectra of dipolar coupled spins and also for the discrimination of enantiomers in weakly aligning media are well known.[110–115] Unlike in dipolar coupled systems where the size of the coupled network of spins depends on their spatial proximity, in isotropic solutions, it depends on the transmission of spin polarization across the chemical bonds. Consequent to the fact that the scalar couplings among protons separated by more than four covalent bonds are most often negligible, the spin system is generally restricted to a smaller size. Therefore, the bigger molecules containing large number of protons may possess several coupled spin systems, which are isolated from one another. In an isolated N coupled spin system, it is possible to selectively excite coherence of higher quantum orders, maximum being the N^{th} quantum. Scalar fields being absent in such a situation, the protons evolve at the sum of their chemical shifts giving a single peak in the N^{th} quantum dimension. As far as the chiral

molecules in the presence of a chiral auxiliary is concerned, two identifiable peaks are detected in the maximum quantum dimension—one for each enantiomer provided there is a measurable difference in their chemical shifts, enabling their discrimination. Another advantage of this method is that the highest quantum dimension is devoid of overlapped peaks from other protons of the molecules and also the huge transition arising from the solvent because of the spin system filtering. The application of such a methodology has been demonstrated for discrimination of chiral molecules in isotropic solutions.[75] The pulse sequence utilized for multiple quantum detection[111] and the cartoon representation of the appearance of the 2D MQ spectrum of a chiral molecule in the presence of a chiral auxiliary are given in Fig. 16.

A number of chiral molecules have been investigated in the presence of different chiral auxiliaries [Fig. 17], and depending on the size of the spin system, appropriate 2nd, 3rd and 4th quantum spectra have been detected to achieve discrimination in the MQ dimension.

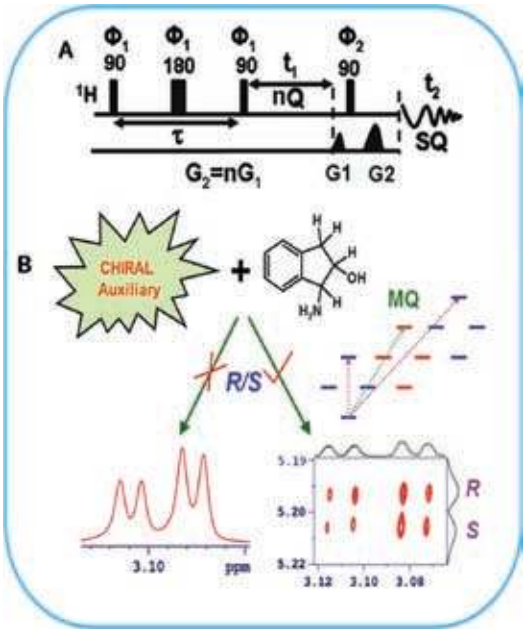

Figure 16: A) The pulse sequence employed for the non-selective excitation of highest quantum coherence of group of scalar coupled spins. The order of the excited quantum is given by n, which depends on the ratio of the gradients G_1 and G_2. The gradient ratio and is set to 1:2, 1:3 and 1:4 for 2nd, 3rd and 4th quantum detection. The phase cycling utilized is $\Phi_1 = \Phi_2 = \Phi_R = 0$. B) Schematic illustration of the appearance of the 2D MQ spectrum of a chiral molecule in the presence of a chiral auxiliary.

5.5 *Use of MQT in diverse situations*

5.5.1 When chiral lanthanide shift reagent is used as an auxiliary: The molecule (*R/S*)-1-phenylethylamine has two aliphatic resonances separated by a large chemical shift difference (bottom trace of Fig. 18A) and a bunch of aromatic resonances. The lanthanide shift reagent europium

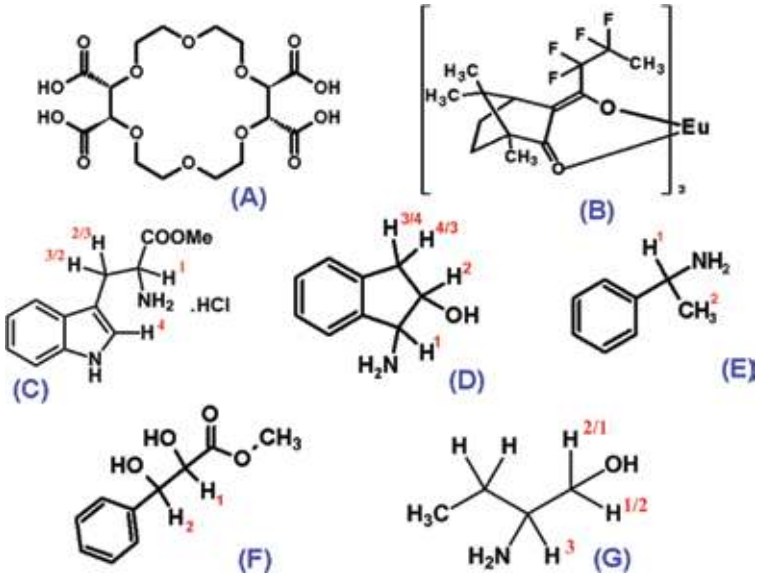

Figure 17: Chemical structures of chiral auxiliaries utilized and the chiral molecules investigated. (18-crown-6)-2,3,11,12-tetracarboxylic acid; A) europium(III)tris[3-(trifluoromethylhydroxymethylene)-(+)-camphorate; B) (*R*/*S*)-tryptophan methyl ester HCl; C) (*R*/*S*)-1-amino-2-indanol; D) (*R*/*S*)-1-phenylethylamine; E) (*R*/*S*)-Methyl-2,3-dihydroxy-3-phenylpropionate; F) and (*R*/*S*)-2-amino-1-butanol; G). The coupled protons numbered in molecules C–G were selectively excited to obtain appropriate highest quantum spectrum.

(III)tris[3-(trifluoromethylhydroxymethylene)-(+)-camphorate has been used to convert enantiomers to diastereomers, and the aliphatic region gave two sets of peaks for both CH and CH_3 groups corresponding to two enantiomers. Though the discrimination is visible, the peaks are partially resolved for their unambiguous assignment to a particular enantiomer (top trace of Fig. 18A). The absence of scalar coupling among CH_3 protons and the existence of scalar coupling between CH and CH_3 groups rendered CH_3 and CH protons to be treated as two coupled spin ½ nuclei, and permitted the detection of DQ-SQ coherence. As expected, the DQ dimension of the two dimensional spectra, reported in Figs. 18B and 18C corresponding to protons H_1 and H_2 respectively, yielded two isolated peaks, one for each enantiomer. The F_2 cross section taken at each frequency in the DQ dimension yielded the corresponding enantiopure spectrum, which pertains to a doublet and a quartet for CH_3 and CH groups respectively. This is clearly visible from the spectrum plotted with enhanced vertical scale (Fig. 18D).

At lower concentrations of the shift reagent there may be indications of discrimination with very poor resolution. Higher concentrations might result in significant broadening of the signal preventing visualization.[116] This situation was encountered in the ^{1}H spectrum of (*R/S*)-Methyl-2,3-dihydroxy-3-phenylpropionate, with 3.2 mM of Europium(III)tris[3-(trifluoromethylhydroxymethylene)-(+)-camphorate. The ^{1}H spectra with and without europium salt and the DQ-SQ spectrum with selective excitation of coupled protons labelled H_1 and H_2 are reported in Fig. 19.

In this molecule the protons H_1 and H_2 form a two coupled spin system of the type AX and gives well dispersed two doublets (bottom trace of Fig. 19A). The use of chiral europium salt resulted in excessive broadening of the spectrum (top trace of Fig. 19A). Thus, instead of achieving larger frequency separations, the peaks get significantly broadened resulting in loss of resolution. Partial resolution is visible in one of the doublets, and the two peaks of other doublet merged into a singlet, precluding any discrimination. Addition of more europium salt is not advantageous as multiplet pattern gets further broadened instead of enhancing their separation. On the other hand, DQ-SQ spectrum has an immediate advantage and the clear differentiation is visible at both the proton sites (Fig. 19B).

5.5.2 When chiral crown ether is used as a chiral auxiliary: In the molecule (*R/S*)-2-amino-1-butanol, the protons identified as H_1, H_2 and H_3 (Fig. 20)

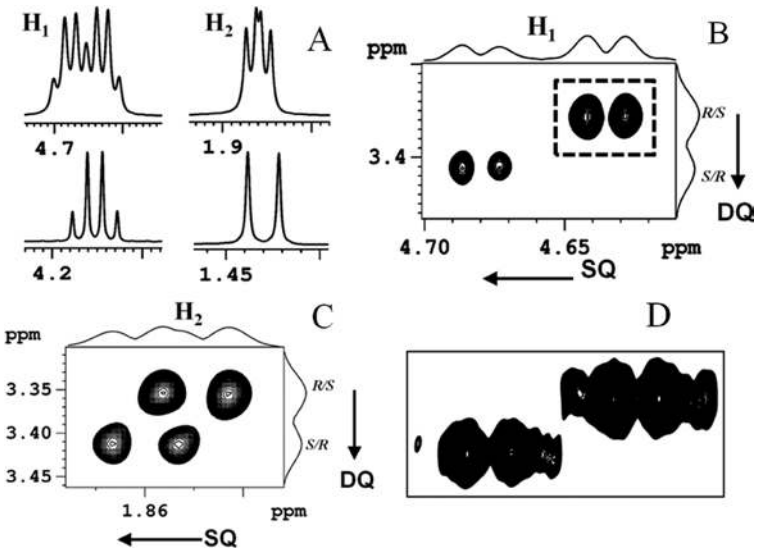

Figure 18: 500 MHz ^{1}H NMR spectra of 117.89 mM (***R/S***)-1-phenylethylamine, with 3.2 mM of chiral europium salt, europium(III)tris[3-(trifluoromethylhydroxymethylene)-(+)-camphorate in the solvent $CDCl_3$; A) bottom trace is the spectrum without lanthanide shift reagent and top trace is with Chiral Lanthanide Shift Reagent; and C) the expanded regions of two dimensional DQ-SQ spectra at the chemical shift positions of protons H_1 and H_2 respectively, obtained with simultaneous excitation of protons CH and CH_3 groups; D) expanded portion of the spectrum marked with broken rectangle in Fig. 18B with enhanced vertical intensity.

form a weakly coupled three spin system of the type AMX. The part of the one dimensional spectrum of this spin system is given in Fig. 20A (bottom trace). The one dimensional spectrum with the utilization of crown ether as an auxiliary contains the superposition of spectrum from both the enantiomers and exhibits the partially resolved multiplet pattern at both the chemical shift positions. Although the discrimination is visible, the degree of discrimination is not sufficient for unambiguous assignment of peaks to each enantiomer. On the other hand, the 3Q (triple quantum)—SQ spectrum, of this molecule with simultaneous flipping of all the three coupled protons gave rise to well resolved peaks, one for each enantiomer in 3Q dimension, while F_2 cross section gave enantiopure spectrum and also clear discrimination in the SQ dimension. This is clearly evident from Figs. 20B and 20C.

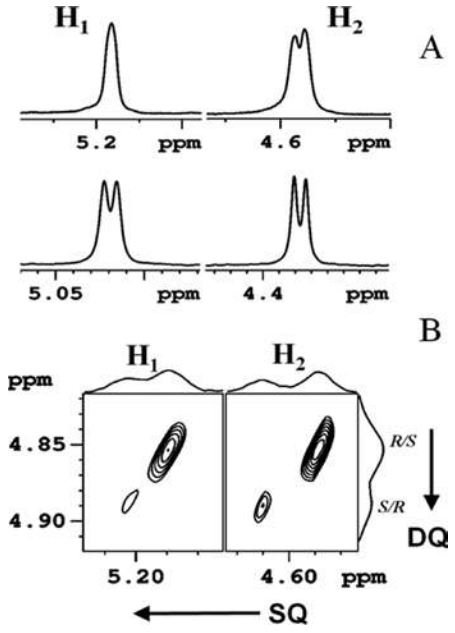

Figure 19: 500 MHz ^{1}H NMR spectra of 59 mM (*R*/*S*)-methyl-2,3-dihydroxy-3-phenylpropionate, with 3.2 mM of europium(III)tris[3-(trifluoromethylhydroxymethylene)-(+)-camphorate in $CDCl_3$ solvent. A) 1D spectra without (bottom trace) and with (top trace) europium salt. B) The regions of 2D DQ-SQ spectra at the chemical shift positions of the protons H_1 and H_2.

5.5.3 Molecules with more than three scalar coupled spins: Each molecule (*R/S*)-tryptophan methylester hydrochloride and (*R/S*)-1-amino-2-indol contains a spin system of four coupled protons. The expanded regions of ^{1}H NMR spectra corresponding to protons $H_{2/3}$ and $H_{3/2}$ of the molecule (*R/S*)-tryptophan methylester hydrochloride and protons H_1, $H_{3/4}$ and $H_{4/3}$ of the molecule (*R/S*)-1-amino-2-indol are given in Figs. 21A and 22A (bottom traces) respectively. The first order analyses of the spectra clearly reveal that in both these molecules four protons are coupled among themselves. The chiral crown ether was utilized to impose diastereomeric interaction. It is evident that in molecule (*R/S*)-tryptophan methylester hydrochloride (top trace of Fig. 21A), the use of chiral crown ether resulted in broadening of peaks and that discrimination is impossible from such a poorly resolved one dimensional spectrum. In the molecule (*R/S*)-1-amino-2-indol, the chemical shift difference between the discriminated peaks is very small (top trace of Fig. 22A) and resulted in

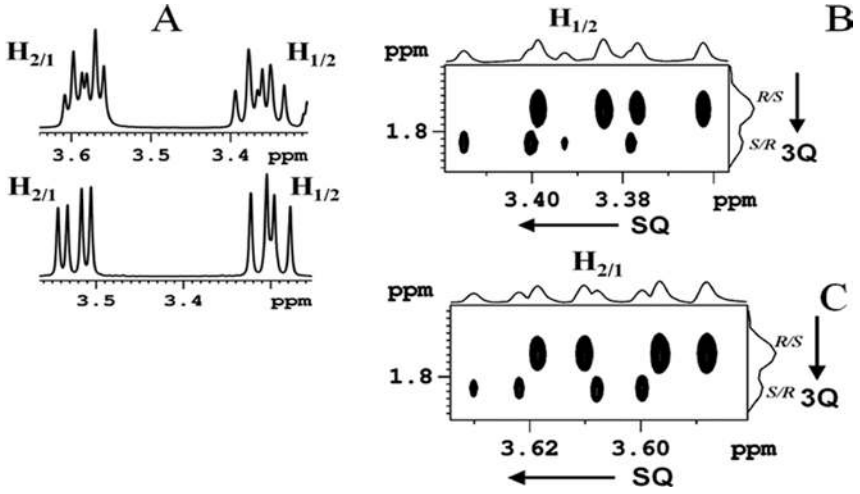

Figure 20: 500 MHz ^{1}H NMR spectra of 128.2 mM (*R*/*S*) - 2-amino-1-butanol with 3.89 mM of (18-crown-6)-2,3,11,12-tetracarboxylic acid, in the solvent MeOD-d_4; A) The 1D spectra without (bottom) and with (top) crown ether, and B) Two dimensional 3Q-SQ spectrum with selective excitation of protons $H_{1/2}$, $H_{2/1}$ and H_3.

poor resolution for two protons H_1 and $H_{4/3}$ and at the proton site ($H_{3/4}$), rendering it is impossible to visualize the discrimination. The two dimensional 4Q (fourth quantum)–SQ spectra reported in Figs. 21B and 21C, and Figs. 22B–22D respectively, for both these molecules gave clear discrimination in the higher quantum dimension. The F_2 cross section taken at the two frequency positions of 4Q dimension resulted in completely unraveled enantiopure spectrum. This discrimination is visible in the direct dimension of 2D spectrum also. The biggest advantage of the MQ-SQ technique is obvious

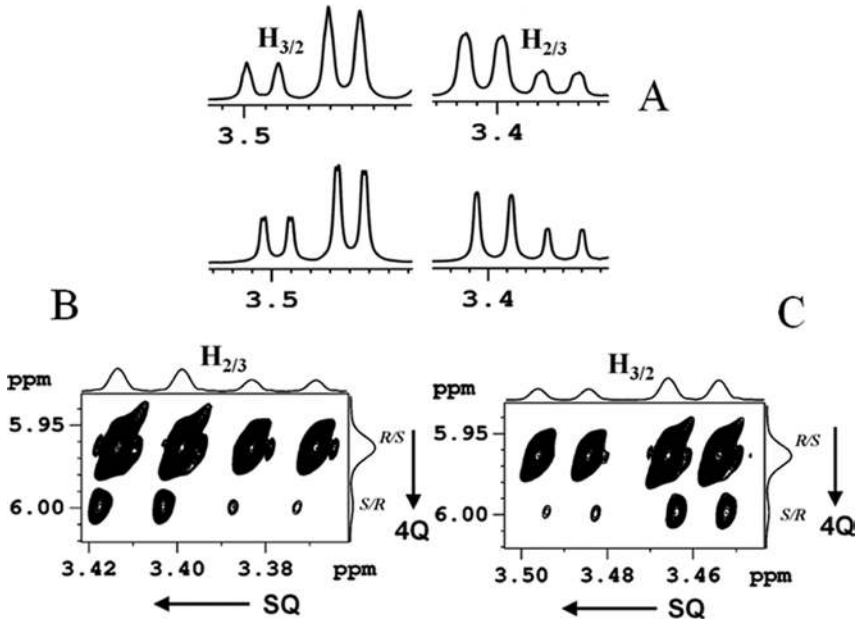

Figure 21: 500 MHz ^{1}H NMR spectra pertaining to the protons $H_{2/3}$ and $H_{3/2}$ of (D/L)-tryptophan methylester hydrochloride (C) (67 mM) with 3.89 mM of (18-crown-6)-2,3,11,12-tetracarboxylic acid (A), in the solvent MeOD-d_4; A) 1D spectrum without (bottom trace) and with crown ether (top trace); B and C) the regions of selectively excited and detected 4Q-SQ spectra pertaining to protons 2 and 3.

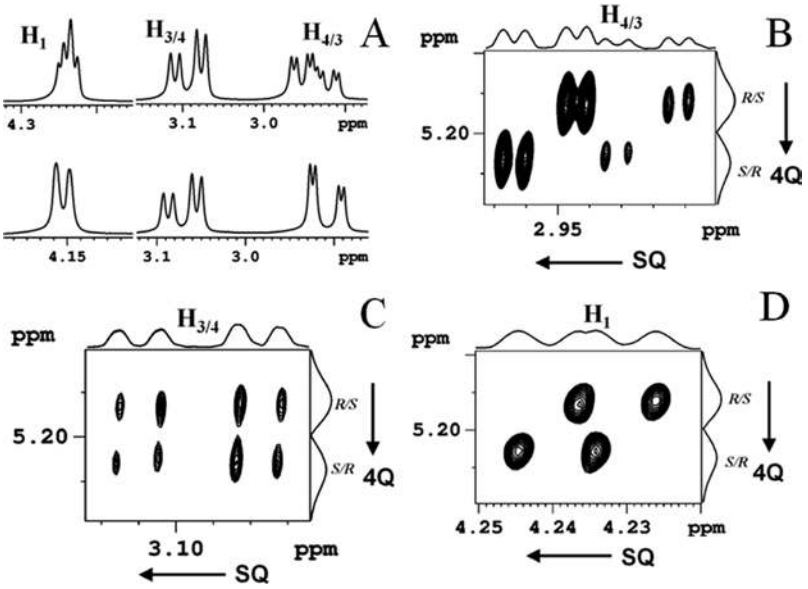

Figure 22: 500 MHz ^{1}H NMR spectra of 137 mM 1-amino-2-indol with 4.5 mM of (18-crown-6)-2,3,11,12-tetracarboxylic acid in the solvent MeOD-d_4; A) 1D spectrum without (bottom trace) and with (top trace) crown ether; B–D) Regions of the 4Q-SQ spectra pertaining to the protons $H_{4/3}$, $H_{3/4}$ and H_1 respectively.

from Fig. 22C, where the discrimination that was impossible to visualize in the 1D spectrum, has been obtained from the 4Q-SQ spectrum. Another important advantage of this methodology is achieving the discrimination at multiple chemical sites.

5.5.4 When more than one scalar coupled spin system is present: When more than one coupled spin network is present in a chosen chiral molecule, depending on the network of the scalar coupled spins, it is possible to excite the appropriate highest quantum coherence to obtain discrimination. This also results in spin system filtering. Therefore, the methodology can be conveniently employed for molecules of larger sizes. The reported MQ-SQ technique also suffers from two limitations, viz., a linear increase in the B_0 field inhomogeneity, and decrease in the sensitivity of detection with the increase in multiple quantum order.

5.5.5 MQ detection and the measurement of enantiomeric excess: The integral areas of the contours of the 2D MQ-SQ spectrum for the discriminated peaks may be utilized to measure enantiomeric excess. However, the method has a limitation for precise measurement, since the intensities of the projections of MQ spectrum are not comparable to that of normal 1D spectrum. This is due to the fact the MQ excitation is maximum for $\tau = 1/4J_{HH}$ and the J values, being different the average delay, has to be utilized. In addition, there may be offset dependence on the intensities and also loss of magnetization due to zero quantum coherence.[77] Therefore, the measurement of enantiomeric excess using multiple quantum methodology may not be precise. However, there are various ways to improve the precision of determinacy, viz., repeating the experiment with several values of τ and co-adding the data,[80,117–120] incrementing the delay with the evolution time t_1,[77] thereby achieving averaging during data acquisition. Another alternative would be to utilize composite excitation and mixing periods to have a uniform effect over a range of coupling constants.[121,122] Therefore, although better discrimination could be achieved using this technique, especially in circumstances when 1D experiments fail, the precise measurement of *ee* would be tedious. Another factor that affects the areas of the contours of the 2D spectrum is the relaxation during multiple quantum excitation period. This factor is also required to be taken into account. As discussed elsewhere,[123] generally the T_1 and T_2 values are nearly identical for the enantiomers within the experimental errors and hence the differential effect, if any, are not reflected on the areas of the contours. Considering various points, the F_1 decoupled experiment could be a better alternative as far as the precise measurement of *ee* is concerned.

6 Utility of Homonuclear *J*-Resolved Technique

All the experiments discussed in the previous sections are restricted to either selective excitation or the excitation of a coupled network of protons. In a recent study[124] the utility of the *J*-resolved experiment for chiral analysis is reported, which does not only involves selective excitation but also circumvents the problem of signal overlap, and the problem of line broadening in the NMR spectrum.

The principle of two dimensional *J*-resolved technique involves the separation of δ and J, and the 2D spectrum reveals the coupling information in F_1 dimension, and together chemical shifts and the couplings in F_2 dimension. The skew projected spectrum obtained by 45° tilting in the F_2 dimension gives proton decoupled proton spectrum or the pure shift spectrum devoid of any multiplet structure in the detection dimension.[125] Schematic illustration of the untilted and 45° tilted 2D spectrum is given in Fig. 23. The F_2 projection of the 2D *J*-resolved spectrum gets simplified and permits the unambiguous enantiodiscrimination and the precise measurement of enantiomeric composition. The experiment is extremely useful on many occasions when simple one dimensional NMR experiment fails to discriminate enantiomers.

For ascertaining the application of *J*-resolved spectroscopy, the molecule 1-aminoindane was investigated using *S*-BINOL as a chiral resolving agent. The chemical structure of this and other investigated molecules and the chiral auxiliaries are reported in Fig. 24. The diastereomer formation involves hydrogen bonded non-covalent interaction.[68,69] The selected regions of one dimensional ^{1}H NMR spectrum, which contains the superposition of peaks from the enantiomers, is reported in Fig. 25 along with the 2D-*J*-resolved spectrum.

It is clear from the top trace of Fig. 25 that the one dimensional spectrum is highly overcrowded even in the presence of the chiral auxiliary hampering the assignment of peaks for two enantiomers and the measurement of difference in their chemical shifts. This spectral complexity arises due to multiplicity pattern and the superposition of spectra of both *R* and *S* enantiomers. The simplification of the spectrum is essential to unambiguously

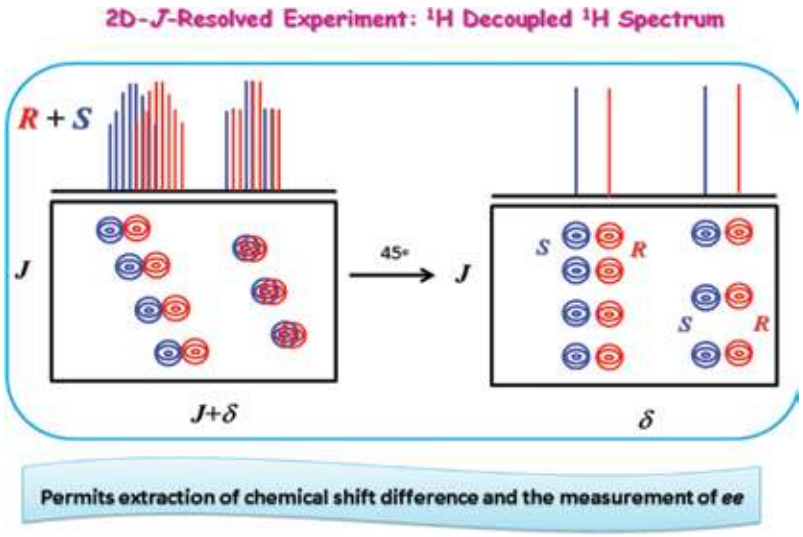

Figure 23: The schematic representation of the *J*-resolved spectrum when the peaks from both the enantiomers are overlapped and their unraveling after obtaining skew projection by 45°.

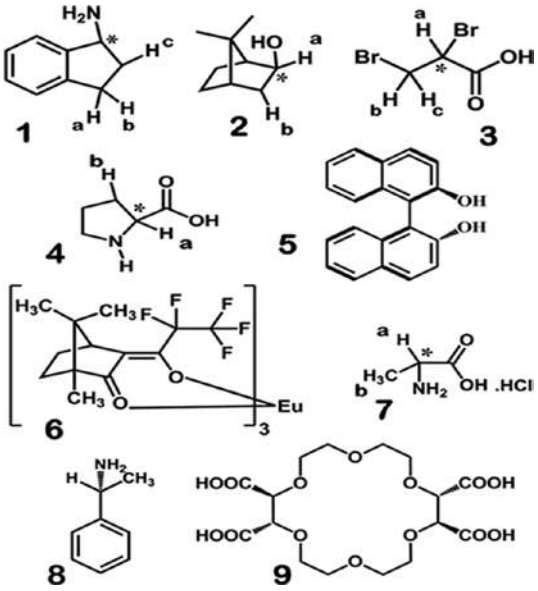

Figure 24: The chemical structures of chiral molecules investigated using *J*-resolved technique; 1-aminoindane (1), exo-norborneol (2), 2,3-dibromopropanoic acid (3), proline (4), alanine hydrochloride (7), and the chiral auxiliaries employed *S*-BINOL (5), Eu(III) complex of d,d-dicamphonylmethane (6), *R*-alphamethylbenzylamine (8), and (+)-(18-crown-6)-2,3,11,12-tetracarboxylic acid (9), The protons labelled with alphabets in the molecules 1, 2, 3, 4 and 7 give discrimination and their chemical shift differences are utilized to test enantiopurity.

discriminate enantiomers, measure their chemical shift difference ($\Delta\delta^{R/S}$), and the determination of enatiomeric excess. Enormous simplification is achieved and the complex multiplet structure is collapsed into a singlet for each enantiomer in the F_2 direction of 45° tilted 2D *J*-resolved spectrum, which gives rise to 'pure shift' spectrum. This facilitated the easy identification of peaks for both the enantiomers, thereby enabling chiral analyses, which otherwise would have been very difficult from the overcrowded one dimensional spectrum.

6.1 *Discrimination using chiral lanthanide shift reagent*

As discussed previously discrimination of enantiomers and the subsequent measurement of *ee* using lanthanide shift reagents are usually difficult.[71,72,116,126] In such complex situations, the *J*-resolved spectroscopy is useful, example of which is demonstrated in testing the enantiopurity of molecule, exo-norborneol. The chiral lanthanide shift reagent, Eu(III) complex of d,d-dicamphonylmethane was utilized to impose diastereomeric interactions. The ^{1}H NMR spectrum of the molecule is reported in Fig. 26, (top trace). It is evident from the expanded regions of the spectrum corresponding to protons a and b, given at the top trace of Fig. 26, that the assignment of peaks for two enantiomers is impossible from this one dimensional spectrum due to severe line broadening. On the other hand, the utilization of 2D *J*-resolved spectrum, given at the bottom of Fig. 26, gave good results and facilitated the visualization of the discriminated peaks.

6.2 *Discrimination using chiral derivatizing agent*

The Chiral Derivatizing Agents are utilized for testing the enantiopurity of chiral primary

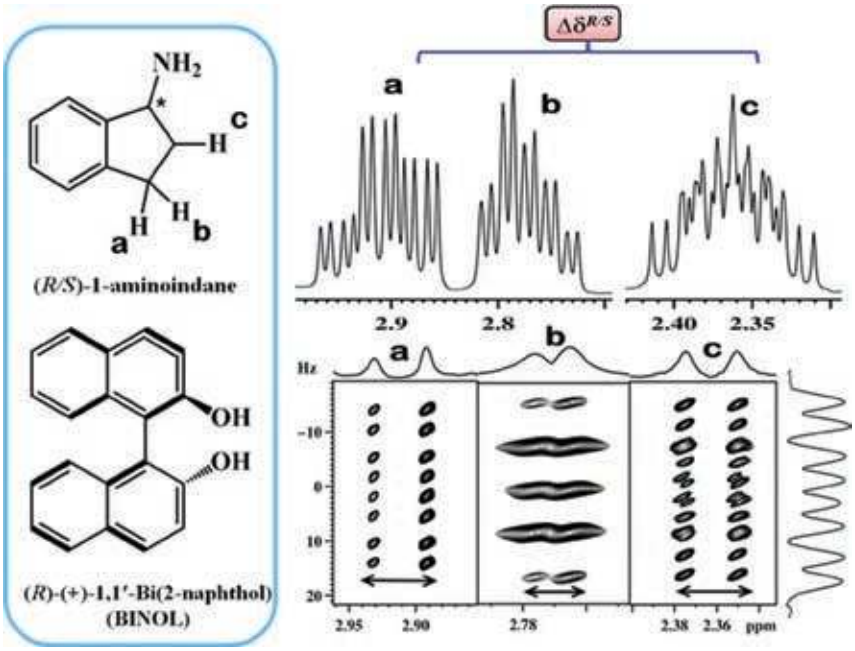

Figure 25: ^{1}H NMR spectrum (upper trace) of 1-aminoindane in the presence of *S*-BINOL (in 1:1 ratio). The a, b and c are the peaks pertaining to protons labelled in the figure given at the top of the spectrum, and the bottom trace is the 45° tilted 2D *J*-resolved spectrum (obtained in the magnitude mode) along with its F_1 and F_2 projections. The chemical structures of the chiral analyte and the chiral auxiliary are also given.

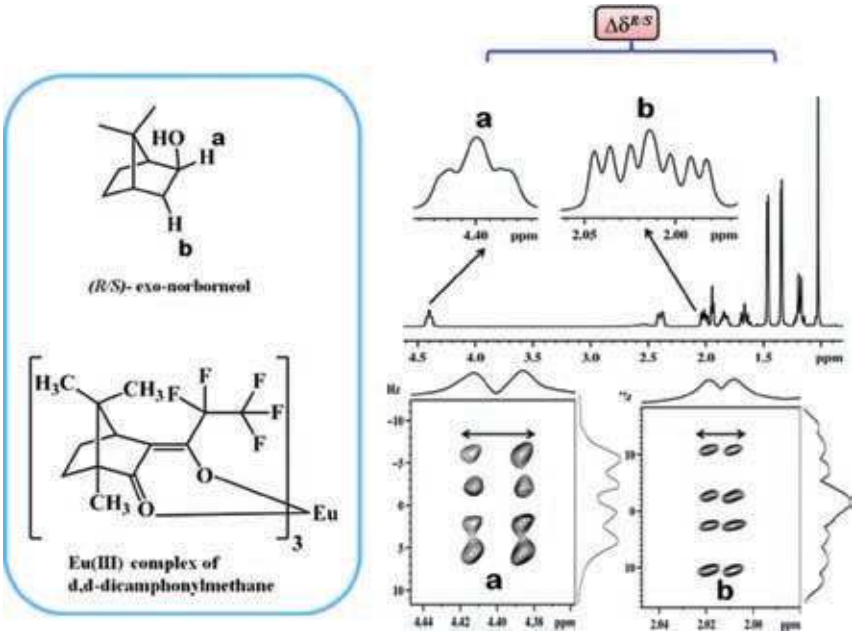

Figure 26: ^{1}H NMR spectrum (upper trace) of exo-norborneol in the presence of Eu(III) complex of d,d-dicamphonylmethane (in 1:1 ratio). The a and b are the peaks pertaining to protons labeled in the figure and the bottom trace is the 45° tilted 2D *J*-resolved spectrum (obtained in the magnitude mode) along with its F_1 and F_2 projections. The chemical structures of the chiral molecule and the auxiliary are also given.

amines, chiral acids and chiral alcohols.[74,127,128] The use of such reagents often suffers from the problems of racemization and kinetic resolution consequent to the small chemical shift difference between the discriminated peaks, thereby hampering chiral analysis and the measurement of *ee*.[129] In the assignment of absolute configuration, accurate value of chemical shift is important and sometimes extraction of the chemical shift value from the ^{1}H-NMR is a difficult task. This

can happen because of overlapping of the peaks of substrate and CDA. The 2D-*J*-resovled experiment approach is advantageous even in such a situation. The utility is demonstrated on the three component derivatization protocols developed for chiral discrimination of amines, chiral hydroxy acids and chiral diacids.[65–67]

6.2.1 Application to secondary butylamine: The three component protocol developed for the discrimination of secondary butylamine is given in Fig. 27.

The aliphatic region the spectrum of secondary butylamine is complex because of multiplicity pattern and the proper baseline resolution could not be achieved, even though the chemical shifts are large, and hence it was difficult to measure precise $\Delta\delta^{R/S}$ (Fig. 28). The 2D-*J*-Resolved experiment yielded accurate $\Delta\delta^{R/S}$, and the corresponding spectrum is reported in Fig. 28.

6.2.2 Testing the enantiopurity of chiral diol using *J*-resolved technique: Another interesting example is demonstrated on iminoboronate esters of 2,4-pentanediol, where the discrimination is achieved at several chemical sites, viz., in the aliphatic region of the spectrum of the molecule and also in the aromatic regions of the diastereomers of iminoboronate esters. The formation of iminoboronate ester of 2,4-pentanediol involves the simple stirring of ternary mixture of 2,4-pentanediol, *R*-alphamethylbenzylamine and 2-formylphenylboronic acid in the solvent $CDCl_3$ and in the presence of 4Å molecular sieves for 15 minutes and the protocol is given in Fig. 29.

The one dimensional spectrum and the 2D *J*-resolved spectrum pertaining to aromatic region of the diastereomers of iminoboronate esters, given in Fig. 30, depict the advantage of the *J*-Resolved technique. The resolution of peaks is essential for

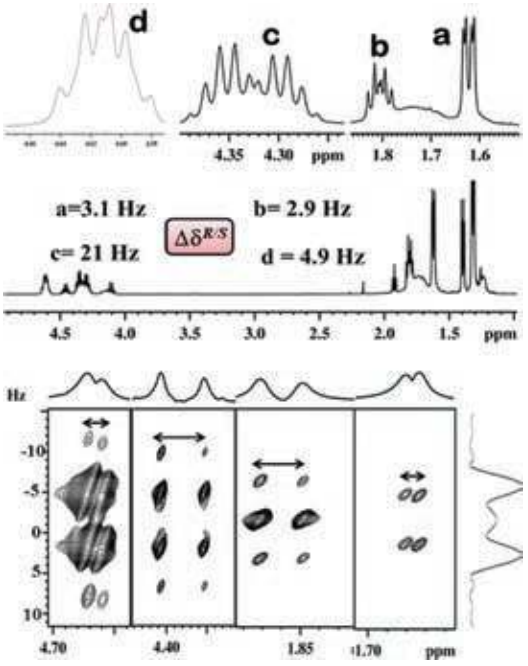

Figure 28: ^{1}H NMR spectrum (top trace) and 2D *J*-resolved spectrum along with F2 projection (bottom trace) of diastereoisomers of iminoboronate esters (*S,R*) and (*S,S*) of secondary butylamine in the solvent $CDCl_3$. Selected regions of the 1D spectrum giving discriminations are expanded, and the $\Delta\delta^{R/S}$ for different protons labelled with alphabets, are also given. Please refer to Fig. 27 for structures of diastereomers.

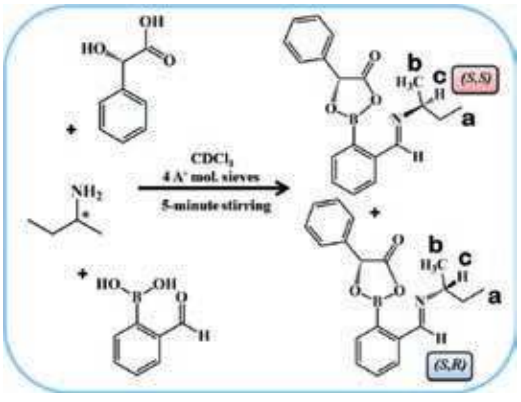

Figure 27: The general scheme involving the three-component reaction of one equivalent each of racemic secondary butylamine, optically pure *S*-mandelic acid and 2-formylphenylboronic acid to obtain diastereomeric iminoboronate esters (*S,R*) and (*S,S*).

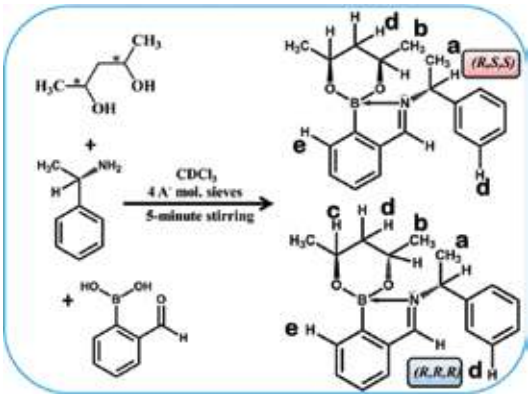

Figure 29: The three-component reaction of one equivalent of racemic 2,4-penatanediol, optically pure *R*-alphamethylbenzylamine and 2-formylphenylboronic acid to give diastereomeric iminoboronate esters (*R,S,S*) and (*R,R,R*).

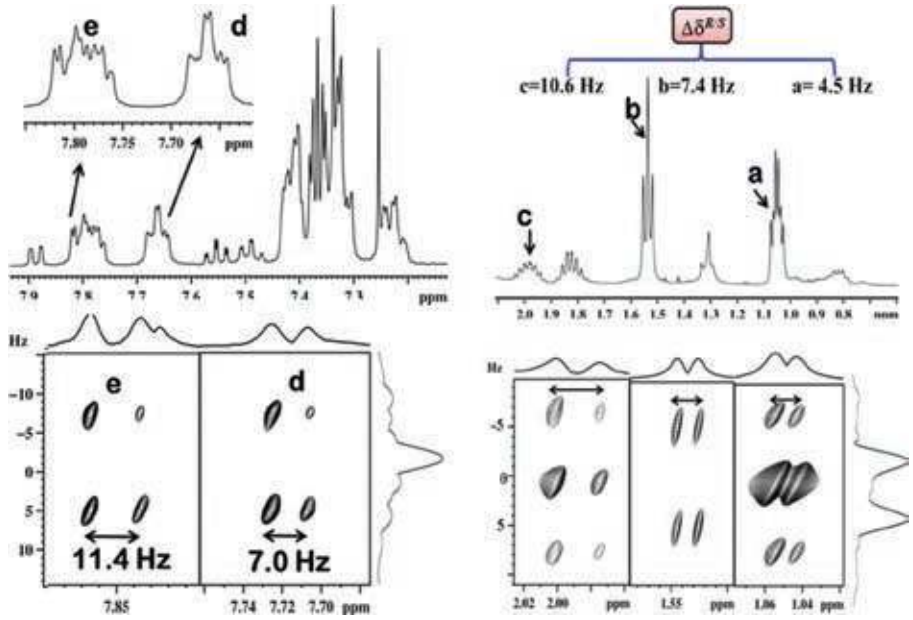

Figure 30: ^{1}H NMR spectrum of 2,4-pentanediol in $CDCl_3$. The 2D-*J* Resolved spectrum is given at the bottom. The expanded aromatic regions of protons of diastereomers of iminoboronate esters (2*R*,4*R*) and (2*R*,4*S*) marked with alphabets d and e, showed discrimination with the chemical shift difference of 11.4 and 7 Hz respectively; Expanded aliphatic region of the spectrum also given, where the 2D *J*-Resolved spectrum yielded discrimination.

the assignment of absolute configuration. Utility of the experiment is clear from the peaks corresponding to proton marked 'e' (given in Fig. 30), where in spite of frequency separation of 11.4 Hz between the discriminated peaks, it was difficult to identify them from the one dimensional spectrum, because of excessive overlap.

The aliphatic region of the spectrum is also given in Fig. 30 along with the chemical shift differences measured at discriminated proton sites. Nonetheless, it was difficult to identify peaks for two diastereomers from the one dimensional spectrum because of excessive overlap. On the other hand, 45° tilted 2D *J*-resolved spectrum (obtained in the magnitude mode) along with its F_1 and F_2 projections aided in the clear identification of diastereomer peaks of iminoboronate esters (2*R*,4*R*) and (2*R*,4*S*).

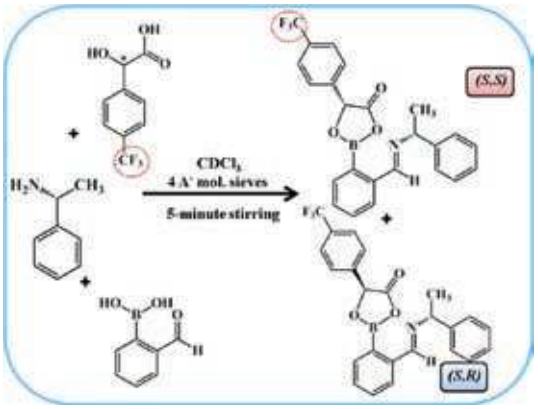

Figure 31: The three-component reaction of one equivalent of racemic 4-trifluoromandelic acid, optically pure S-alphamethylbenzylamine and 2-formylphenylboronic acid to give diastereomeric iminoboronate ester (S, R) and (S, S).

6.3 *Application to ^{19}F–NMR*

To derive the benefit of large chemical shift dispersion, high natural abundance and larger sensitivity, ^{19}F NMR spectrum has been utilized for measuring enantiopurity.[67] At times the improper base line correction between the discriminated peaks might give erroneous results, especially when one is interested in the determination of enantiomeric composition. The two dimensional *J*-resolved experiment can be employed in such situations. An example of such a situation was encountered in the ^{19}F NMR spectrum of 4-trifluoromethylmandelic acid where the CF_3 group is situated far away from the stereogenic centre. The preparation of iminoboronate ester involved stirring ternary mixture of racemic 4-trifluoromethyl mandelic acid, 2-formylphenyl boronic acid and *R*-alphamethylbenzylamine one equivalent each in solvent $CDCl_3$. The protocol for iminoboronate formation is given in Fig. 31.

The one dimensional ^{19}F NMR spectrum failed to give high the resolution required for

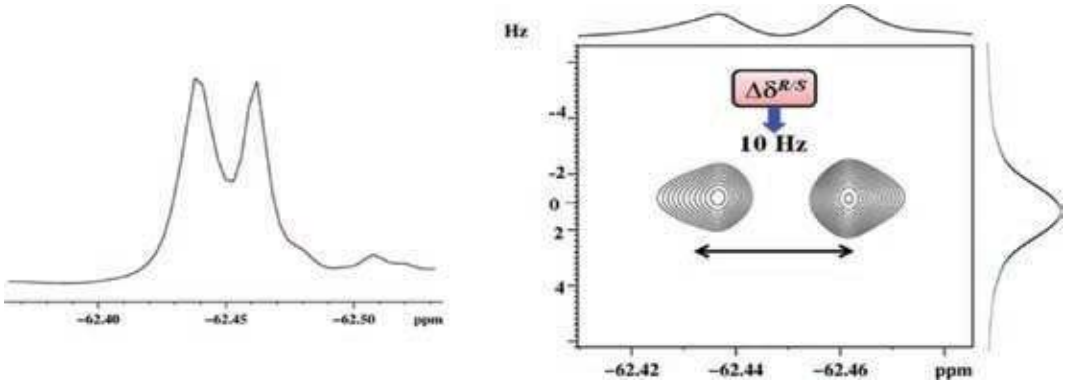

Figure 32: ^{19}F NMR spectrum (left trace) and the corresponding 2D *J*-resolved spectrum along with F_2 projection (right trace) of diastereoisomers of iminoboronate esters (*S,R*) and (*S,S*) of 4-trifluoromethylmandelic acid in the solvent $CDCl_3$.

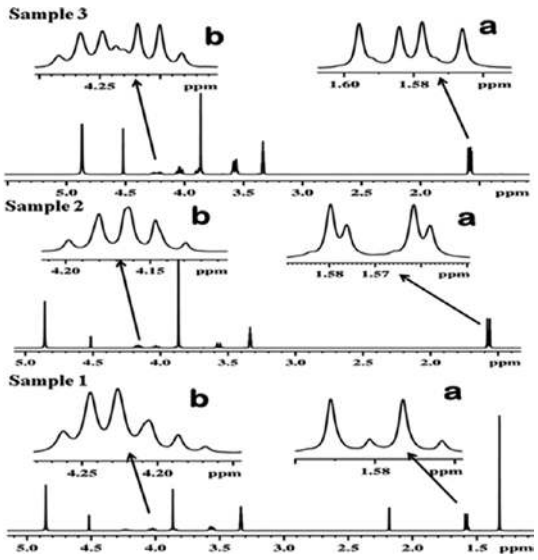

Figure 33: ^{1}H-NMR spectrum of alanine hydrochloride in the presence of (+)-(18-crown-6)-2,3,11,12-tetracarboxylic acid. Sample 1; D/L: 10 mg and 10 mg of 18-crown-6; sample 2; D/L: 13.1 mg and 7.8 mg of 18-Crown-6; sample 3; D/L: 16.7 mg and 3.7 mg of 18-Crown-6. a and b peaks are marked and the corresponding alphabet labelling in the structure are given in Fig. 24.

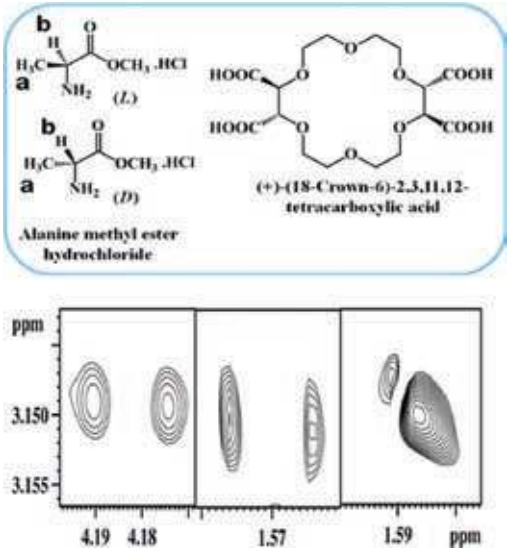

Figure 34: ^{1}H-2D *J*-resolved NMR spectrum (obtained in the magnitude mode) of alanine hydrochloride with (+)-(18-Crown-6)-2,3,11,12-tetracarboxylic acid. Sample 1, D/L: 10 mg and 10 mg 18-Crown-6; sample 2, D/L: 13.1 mg and 7.8 mg 18-Crown-6; sample 3, D/L: 16.7 mg and 3.7 mg 18-Crown-6. The stock solutions were prepared in 2 ml of methanol-D_4. For samples 1 and 3 the CH_3 group (marked b) and for sample 1 CH group (marked a) of the molecule were monitored. The chemical structure of the chiral molecule and the chiral auxiliary along with the alphabet labelling are given at the top.

measurement of *ee* since the spectrum is partially resolved. On the other hand, in the 2D *J*-resolved spectrum the peaks are clearly distinguished permitting the accurate measurement of *ee*. The corresponding ^{19}F NMR spectrum is given in Fig. 32.

The chemical shift difference between the discriminated peaks could be precisely measured from the 2D spectrum. Because of improper base line resolution the measured enantiomeric excess *(ee)* from the one dimensional spectrum is likely to be imprecise. However, this problem is circumvented by the utility of 2D spectrum.

6.4 *J-Resolved technique and enantiomeric excess*

The utility of the 2D *J*-resolved spectroscopy for the precise measurement of *ee* has been

Table 1: The enantiomeric excess measured from the proton 2D *J*-Resolved spectrum of alanine hydrochloride for gravimetrically prepared samples of different scalemic ratios.

Entry	Proton chosen	$^{R/S}$ (Hz)	Integration (*D*):(*L*) I_D:I_L	Experimental *ee*%	Gravimetrically prepared with excess of *D*
Sample 1	CH_3	4.7	1.0:0.60	25 ± 1.6	25.8
Sample 2	CH_3	2.2	1.0:0.22	64 ± 0.3	63.7
Sample 3	CH_3	20.0	1.0:0.0050	99 ± 0.5	98.0

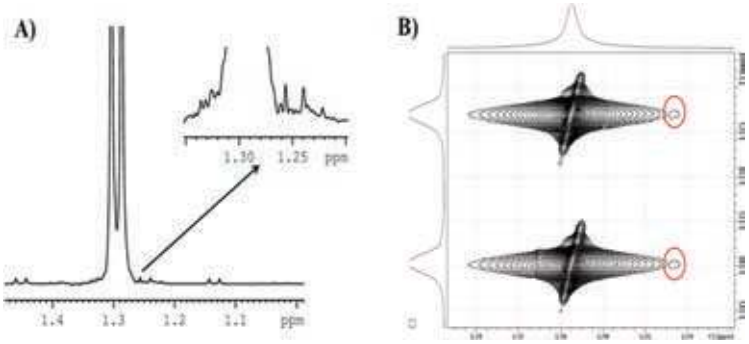

Figure 35: A) 1D ^{1}H-NMR spectrum and B) 2D *J*-resolved spectrum of alanine hydrochloride and (+)-(18-Crown-6)-2,3,11,12-tetracarboxylic acid with 98% in excess of D form. The peak corresponding to the methyl group is given. The marked circles identify the spectrum from *L* enantiomer.

explored by studying the molecule alanine hydrochloride, in the presence of chiral crown ether, (+)-(18-Crown-6)-2,3,11,12-tetracarboxylic acid, at different scalemic ratios of enantiomers (samples 1–4). The one dimensional ^{1}H-NMR spectra for different samples 1, 2 and 3 prepared with different enantiomeric ratio are reported in Fig. 33. The careful inspection of the spectrum reveals that the peaks from each enantiomer are severely overlapped without any proper baseline correction, prohibiting the precise measurement of *ee*. In order to resolve such a problem the ^{1}H-detected 2D-*J*-Resolved experiments have been carried out. The 2D *J*-resolved spectra of chosen regions are reported in Fig. 34 and the enantiomeric excess data is reported in Table 1.

For enantiomeric analysis in Sample 2, the CH peak has been chosen, and for the remaining two samples CH_3 peaks have been chosen. Measured *ee* reported in Table 1 confirms that they agree with gravimetrically prepared samples within experimental error. For ascertaining the lowest *ee* that one can determine by this method, another solution with 2% excess of *D* has been studied (sample 4). The spectrum is reported in Fig. 35. Even for this sample the measured *ee* agreed with gravimetrically prepared sample within experimental error. It is conclusively evident that 2D experimental method is very promising for chiral analyses in isotropic solutions, and can be applied in difficult and complicated situations when the spectra are severely overlapped or overcrowded, or complex, even with the utilization of solvating, derivatizing and lanthanide shift reagents.

7 Pure Shift NMR

Number of experiments based on homodecoupling, which removes multiplicity pattern, circumventing the limitations of spectral resolution, where the information on the coupling constants are lost have been reported. Such broad band homodecoupling experimental sequences, cited as pure shift NMR, have been appropriately modified to derive specific information.[130–136] The broadband homdecoupled ^{1}H NMR spectrum results in complete proton decoupled proton spectrum, where multiplicity arising due to various coupling interactions is completely removed, yielding only a single peak at the respective chemical shift positions of each chemically distinct proton. The advantage of such pure shift approach is the dramatic improvement in spectral resolution. The most widely used decoupling techniques are BIlinear Rotation Decoupling (BIRD), and the spatial and frequency selective refocusing techniques.[55,137–140] While measuring the enantiomeric/diastereomeric ratios, it is sufficient to monitor one or two selected peaks which give better chemical shift separations. In such situations, the band selective version of pure shift technique can be employed.[141–143]

The experiments involving homonuclear broad band decoupling during acquisition also gives enhanced sensitivity and resolution.[135,144,145] The utility of band selective pure shift experiment has been reported for measurement of diastereomeric ratios in two examples, viz., flavanone glycoside hesperidin and diastereomeric oligomeric products of an enamide addition reaction resulting in 1,61-asymmetric induction.[136,142] The selected region of the conventional one dimensional spectrum of this molecule exhibited a number of overlapped multiplet peaks, which collapsed into two individual singlets at the chemical shift positions that permitted the measurement of diastereomeric ratio.

Another experiment that involves frequency selective broadband homo decoupling was demonstrated, which again resulted in complete removal of scalar couplings and gave two peaks pertaining to each diastereomer, at their respective chemical shift positions. The technique was applied for enantiodiscrimination on two molecules, (*R/S*)-ibuprofen, where β-cyclodextrin was used as a chiral solvating agent and in (*R,S*)-1-aminoindan in the presence of (*R*)-(-)-1-(9-anthryl)-2,2,2-trifluoroethanol as the chiral solvating agent.[146]

8 Conclusions

The inherent problems encountered in the chiral analyses using ^{1}H NMR spectroscopy is the severe overlap of peaks due to small chemical shift difference between discriminated peaks, line broadening in case of metal complexes, and the presence of unreacted substrates (impurities). Use of large quantities of chiral solvating agents or lanthanide shift, though helps in discrimination, causes excessive line broadening and its utility beyond certain ratio of substate to resolving agent, has very little impact. In overcoming such problems, a number of experiments have been developed, which includes, frequency selective homodecoupling, band selective homodecoupling, broadband homodecoupling, etc. All these experiments effectively remove the scalar couplings and give a singlet at the respective chemical shift positions of the discriminated peaks. Some of these experiments also find utility in the complete unraveling of the enantiopure spectra, precise measurement of enantiomeric excess, even in the presence of unreacted species present in the sample. In addition, the judicial use of the well known two dimensional experiments also aid in overcoming the spectral complexity. The present review gives a comprehensive account of the recently introduced new NMR experiments for enantiodiscrimination, in isotropic solutions, with a special emphasis on the work carried out by authors group.

Acknowledgements

Sachin Rama Chaudhari would like to thank Indian Institute of Science for RA. NS gratefully acknowledges the generous financial support by the Science and Engineering Research Board, New Delhi (Grant No. SR/S1/PC-42/2011) and Board of Research in Nuclear Sciences (Grant No. 2013/37C/4/BRNS).

Received 23 June 2014.

References

1. Eliel, E. L., (1962) *Stereochemistry of Carbon Compounds*, McGraw-Hill Book Co.
2. Morris, D. G., (2001) *Stereochemistry*, The Royal Society of Chemistry, Cambridge.
3. Robinson, M. J. T., (2001) *Organic Stereochemistry* (Oxford Chemistry Primers), Oxford University Press, New York.
4. Kalsi, P. S., (2005) *Stereochemistry, Conformation and Mechanism* 6th Edition, New Age International Pvt. Ltd., New Delhi.
5. Cahn, R. S., Ingold C and Prelog V. (1966) *Angew. Chem.* Int. Ed. Engl., 5, 385.
6. Cahn, R. S. and Ingold C. K., (1951) *J. Chem.* Soc. 612.
7. IUPAC Commission on Nomenclature of Organic Chemistry, 1974 recommendations for section E, Fundamental Stereochemistry, (1976) Pure Appl. Chem., 45, 11.
8. Nasipuri, D., (2009) *Stereochemistry of Organic Compounds, Principles and Applications*, 2nd Edition, New Age International (P) Ltd.
9. Gupta, S. S., (1997) Basic Stereochemistry of Organic Molecule, Book Syndicate Private Ltd.
10. Cairns, D., (2008) Essentials of Pharmaceutical Chemistry, Third edition, Pharmaceutical Press, USA.
11. Ikai, T., Okamoto Y. (2009) Chem. Rev. 109, 6077.
12. Parker, D., (1991) Chem. Rev., 91, 1441.
13. Dunitz, J. D., (1995) *X-Ray Analysis and the Structure of Organic Molecules*, 2nd Corrected Reprint; Verlag Helvetica Chimica Acta, Basel and VCH: New York.
14. Harada, N., Nakanishi K. (1983) *Circular Dichroic Spectroscopy-Exciton Coupling in Organic Stereochemistry*, University Science Book: Mill Valley, CA.
15. Minick, D. J., Copley, R. C. B., Szewczyk, J. R., Rutkowske, R. D., Miller, L. A., (2007) *Chirality*, 19, 731.
16. Stephens, P. J., Pan, J. J., Krohn, K., (2007) *J. Org. Chem.*, 72, 7641.
17. Ward, T. J., Hamburg, D. M., (2004) *Anal. Chem.*, 76, 4635.
18. Ward, T. J., Ward, K. D., (2010) *Anal. Chem.*, 82, 4712.
19. Sekhon, B. S., *Int. J. Pharm Tech. Res.*, (2010) 2, 1584–1594.
20. Mateos, J. L., Cram, D. J., (1959) *J. Am. Chem. Soc.*, 81, 2756.
21. Wenzel, T. J., (2007) *Discrimination of Chiral Compounds Using NMR Spectroscopy*, Wiley Interscience, Hoboken, NJ.

22. Seco, J. M., Quinoa, E., Riguera, R., (2004) *Chem. Rev*. 104, 17.
23. Wenzel, T. J., Chisholm, C. D., (2011) *Prog. Nucl. Magn. Reson. Spectrosc*. 59, 1.
24. Sarfati, M., Lesot, P., Merlet, D., Courtieu, J., (2000) *Chem. Commun*. 2069.
25. Lokesh, Suryaprakash, N., (2013) *Chem. Comm*., 49, 2049.
26. Lokesh, Suryaprakash, N., (2012) *Chem. Eur. J*., 18, 11560.
27. Reddy, U. V., Suryaprakash, N., (2011) *Chem. Comm*., 47, 8364.
28. Luy, B., Kobzar, K., Kessler, H., (2004) *Angew. Chem*. 116, 1112; Angew. Chem. Int. Ed. (2004) 43, 1092.
29. Luy, B., Kobzar, K., Knör, S., Furrer, J., Heckmann, D., Kessler, H., (2005) *J. Am.Chem. Soc.*127, 6459.
30. Kummerlöwe, G., Knör, S., Frank, A. O., Paululat, T., Kessler, H., Luy, B., (2008) *Chem. Commun.* 44, 5722.
31. Luy, B., (2010) *J. Ind. Inst. Sci.,* 90, 119 and references therein.
32. Meddour, A., Canet, I., Loewenstein, A., Pechine, J. M., Courtieu, J., (1994) *J. Am. Chem. Soc.,* 116, 9652.
33. Chalard, P., Bertrand, M., Canet, I., Thery, V., Remuson, R., Jaminet, G., (2000) *Org. Lett.,* 2, 2431.
34. Lesot, P., Courtieu, J., (2009*) Prog. Nucl. Magn. Reson. Spectrosc.* 55, 128.
35. Raban, M., Mislow, K., (1965*) Tetrahedron Lett.,* 48, 4249.
36. Pirkle, W. H., (1966) *J. Am. Chem. Soc.,* 88, 1837.
37. Jeffrey, G. A., (1997) *An Introduction to Hydrogen Bonding, Oxford University Press, Oxford.*
38. Schneider, H.-J., Yatsimirsky A., (2000) *Principles and Methods in Supramolecular Chemistry,* Wiley, New York.
39. Pirkle, W. H., Hoover, D. J., (1982) *Top. Stereochem.* 13, 263.
40. Hinckley, C. C., (1969*) J. Am. Chem. Soc.*, 91, 5160.
41. Farjon, J., Baltaze J. P., Lesot P., Merlet D., Courtieu (2004) J. *Magn. Reson. Chem.,* 42, 594.
42. Dale, J. A., Mosher H. S. (1973*) J. Am. Chem. Soc.,* 95, 512.
43. Dale, J. A., Dull D. L., Mosher H. S., (1969) *J. Org. Chem.,* 34, 2543.
44. Uccello-Barretta, G., Bernardini, R., Balzano, F., Salvadori, P., (2002) *Chirality*, 14, 484.
45. Nieto, S., Cativiela, C., Urriolabeiti, E. P., (2012) *New J. Chem.,* 36, 566.
46. Rodrıguez-Escrich, S., Popa, D., Jimeno, C., Vidal-Ferran, A., Pericas, M. A., (2005) *Org. Lett.*, 7, 3829.
47. Orlov, N. V., Ananikov, V. P., (2010) *Chem. Commun.,* 46, 3212 and references therein.
48. Nath, N. and Suryaprakash, N., (**2010**) *J. Magn. Reson, 202,* 34.
49. Uday, R. P., Bikash, B., Suryaprakash, N., (2008*) J. Phys. Chem. A.*, *112*, 5658.
50. Uday, R. P., Suryaprakash, N., (2008*) J. Magn. Reson.*, *195*, 145.
51. Uday, R. P., Suryaprakash, N., (2010) *J. Magn. Reson. 202*, 217.
52. Aue, W. P., Karhan, J., Ernst, R. R., (1976) *J. Chem. Phys. 64*, 4226.
53. Farjon, J., Merlet, D., Lesot, P., and Courtieu, J., (2002) *J. Magn. Reson. 158*, 169.
54. Uday, R. P., Bikash, B., Suryaprakash, N. (2008) *J. Magn. Reson. 191*, 259.
55. Giraud, N., Joos, M., Courtieu, J., Merlet D., (2009) *Magn. Reson. Chem. 47*, 300.
56. Uday, R. P., Suryaprakash, N., (2010) *J. Phys. Chem. A*, *114,* 5551.
57. Nath, N., Kumari, D., Suryaprakash, N., (2011) Chem. Phys. Letts. 508, 149.
58. Oliver, M., Bach II, A., Balibar, C., Byrne, N., Cai, Y., Carter, G., Chlenov, M., Di, L., Fan, K., Goljer, I., He, Y., Herold, D., Kagan, M., Kerns, E., Koehn, F., Kraml, C., Marathias, V., Marquez, B., McDonald, L., Nogle, L., Petucci, C., Schlingmann, G., Tawa, G., Tischler, M., Williamson, R. T., Sutherland, A., Watts, W., Young, M., Zhang, M.Y, Zhang, Y., Zhou, D. and Ho, D., (2007) *Chirality*, 19, 658.
59. Klika, K. D., (2009) *Tetrahedron: Asymm.,* 20, 1099.
60. Lovely, A. E., T. Wenzel, (2006) *Org. Lett.*, 8, 2823.
61. Lokesh, Chaudhari, S. R. and Suryaprakash, N., *Org. Biomol. Chem*., (2014) 12, 993.
62. Wenzel, T. J. and Chisholm, C. R., (2011) *Chirality*, 23, 190.
63. Seco, J. M., Quiñoá, E., Riguera, R., (2012) *Chem. Rev*., 112, 4603.
64. Seco, J. M., Quiñoá E., R. Riguera, (2004) *Chem. Rev*., 104, 17.
65. Pérez-Fuertes, Y., Kelly, A. M., Johnson, A. L., Arimori, S., Bull, S. D., and James, T. D., (2006) *Org. Lett*., 8, 609.
66. Chaudhari, S. R. and Suryaprakash, N., (2012) *J. Org. Chem.,* 77, 648.
67. Chaudhari, S. R. and Suryaprakash, N., (2012) *Org. Biomol. Chem.,* 10, 6410.
68. Tanaka, K., Ootani, M., Toda, F., (1992) *Tetrahedron: Asymmetry*, 3, 709.
69. Toda, F., Mori, K., Sato, A., (1988) *Bull. Chem. Soc. Jpn.,* 61, 4167.
70. Lovely, A. E., Wenzel, T. J., (**2006**) *J. Org. Chem.,* 71, 9178.
71. Wenzel, T. J., (1978) NMR Shift Reagents, *CRC Press, Inc: Boca Raton,* FL.
72. McCreary, M. D., Lewis, D. W., Wernick, D. L., Whitesides, G. M., (1974) *J. Am. Chem. Soc.* 96, 1038.
73. Cuevas, F., Ballester, P., Pericás, M. A. (**2005**) *Org. Lett*., 7, 5485.
74. Yang, D., Li, X., Fan, Y. F., Zhang, D.W., (**2005**) *J. Am. Chem. Soc*. 127, 7996.
75. Kumari, D., Hebbar, S., Suryaprakash, N., (2013) *RSC Adv*., 3, 3071.
76. Braunschweiler, L., Bodenhausen, G. and Ernst, R.R., (1983) *Mol. Phys*., **48**, 535.
77. Norwood, T. J., (1992) *Prog. NMR Spectroscopy*, *24,* 295.
78. Bodenhausen, G., (**1980**) *Prog. NMR Spectrosocpy, 14,* 137.
79. Warren, W. S., Pines, A., (1981) *J. Am. Chem. Soc*., **103**, 1613.

80. Warren, W. S., Murdoch, J. B., Pines, A., (1984) *J. Magn. Reson*., **60**, 236.
81. Warren, W. S., Pines A., (1981) *J. Chem. Phys.,* **74**, 2808.
82. Warren, W. S., Pines, A. (1982) *Chem. Phys. Letts*., **88**, 441.
83. Weitekamp, D. P., Garbow, J. R., Pines, A., (1982) *J. Chem. Phys.,* **77**, 2870.
84. Murdoch, J. B., Warren, S. W., Weitekamp, D. P., Pines, A., (1984) *J. Magn. Reson.,* **60**, 205.
85. Munowitz, M., Pines, A., (1986) *Science*, **233**, 525.
86. Murali, N., Ramakrishna, Y. V. S., Chandrasekhar, K., Thomas, M. A., and Kumar, A., (1984) *Pramana*, **23**, 547.
87. Permi, P., Annila, A., (2000) *J. Biomol. NMR*, **16**, 221.
88. Meissner, A., Duus, J. Ø, and Sørensen, O. W., (1997) *J. Magn. Reson.,* **128**, 92.
89. Meissner, A., Duus, J. Ø., and Sørensen, O.W., (1997) *J. Biomol. NMR*, **10**, 89.
90. Sørensen, M. D., Meissner, A., Sørensen, O.W., (1997) *J. Biomol. NMR*, **10**, 181.
91. Meissner, A., Herbrüggen, T. S., Sørensen, O. W., (1998) *J. Am.Chem. Soc*., **120**, 3803.
92. Briand, J., Sørensen, O. W. (1998) *J. Magn. Reson.,* **135**, 44.
93. Nolis, P., and Parella, T., (2007) *J. Biomol. NMR,* **37**, 65.
94. Duma, L., Hediger, S., Lesage, A. and Emsley, L., (2003) *J. Magn. Reson*., **164**, 187.
95. Nolis, P., Espinosa, J. F., Parella, T., (2006) *J. Magn. Reson*., **180**, 39.
96. Parella, T, Gairi, M., (2004) *J. Am. Chem. Soc.,* **126**, 9821.
97. Guichard, G., Violette, A., Chassaing, G., Miclet, E., (2008) *Magn. Reson. Chem*., **46**, 918.
98. Rexroth, A., Schmidt, P., Szalma, S., Geppert, T., Schwalbe, H., Griesinger, C., (1995) *J. Am. Chem. Soc*., **117**, 10389.
99. Anderson, P., Weigelt, J., Otting, G., (1988) *J. Biomol. NMR*, **12,** 435.
100. Brutscher, B., (2001) *J. Magn. Reson.,* **151**, 332.
101. Permi, P., (2003) *J. Magn. Reson.,* **163**, 114.
102. Duma, L., Hediger, S., Brutscher, B., Böckmann, A., and Emsley, L., (2003) *J. Am. Chem. Soc*., **125,** 11816.
103. Verel, R., Manolikas, T., Siemer, A. B., Meier, B. H., (2007) *J. Magn. Reson*., **184**, 322.
104. Permi, P., Annila, A., (2001) *J. Biomol. NMR,* **20**, 127.
105. Permi, P., (2002) *J. Biomol. NMR*. **22,** 27.
106. Lee, D., Vögeli, B., Pervushin, K., (2005) *J. Biomol. NMR*, **31**, 273.
107. Würtz, P., Fredriksson, K., Permi, P., (2005) *J. Biomol. NMR*, **31**, 321.
108. Rani, G. C. R., Riek, R., (2003) *J. Am.Chem. Soc.,* **125**, 16104.
109. Vasos, P. R., Hall, J. B., Fushmann, D., (2005) *J. Biomol. NMR*, **31,** 149.
110. Bikash, B, Suryaprakash, N. J. (2007) *Chem. Phys.* 127, 214510.
111. Lesot, P., Merlet, D., Courtieu, J., Emsley, J. W., (1996) *Liq. Cryst*. 21 427.
112. Bikash, B., Uday R. P., Suryaprakash, N., (2007) *J. Phys. Chem. B,* 111, 12403.
113. Bikash, B., Uday, R.P., Suryaprakash, N., (2008) *J. Magn. Reson*, 192, 101.
114. Bikash, B., Uday, R.P., Suryaprakash, N., (2008) *J. Magn. Reson*, 192, 92.
115. Nath, N., Bikash, B., Suryaprakash, N. (2009) *J. Magn. Reson*, 200, 101.
116. Bikash, B., Uday, R.P., Suryaprakash, N., (2009) *Ann. Rep. NMR Spectroscopy*, Graham A. Webb., The Netherlands: Elsevier, 67, 331.
117. Sweeting, L. M., Crans, D. C., Whitesides, G. M. (1987) *J. Org. Chem*., 52, 2273.
118. Weitekamp, D. P. (1983) *Adv. Magn. Reson*. 11, 111.
119. Weitekamp, D. P., Garbow J. R., Pines, A. (1982) *J. Magn. Reson*. 46, 529.
120. Sørenson, O. W., Levitt M. H., Ernst R. R., (1983) *J. Magn. Reson*. 55, 104.
121. Rance, M., Sørensen, O. W., Leupin, W., Kogler, H., Wüthrich, K., Ernst R. R., (1985) *J. Magn. Reson.* 61, 67.
122. Munowitz, M., Pines, A., (1987) *Adv. Chem. Phys*. 66, 1.
123. Barbara, T. M., Tycko, R., Weitekamp, D. P., (1985) *J. Magn. Reson.,* 62, 54.
124. Nath, N., Suryaprakash, N., (2011) *Chem. Phys. Letts*., 502, 136.
125. Chaudhari, S. R., Suryaprakash, N., (2013) *Chem. Phys. Letts*. 555, 286.
126. Claridge, T. D. W., (2009) *High-Resolution NMR Techniques in Organic Chemistry*, Tetrahedron Organic Chemistry Series, Vol. 27, Second Ed.
127. Wenzel, T. J., Ciak, J. M., (**2004**) *Electronic Encyclopedia of Reagents for Organic Synthesis. John Wiley & Sons, Ltd: Sussex, UK.*
128. Yang, X., Wang, G., Zhong, C., Wu, X., Fu, E., (**2006**) *Tetrahedron: Asymm.*,17, 916.
129. Yang, D., Li X., Fan, Y. F., Zhang, D. W., (**2005**) *J. Am. Chem. Soc.,* 127, 7996.
130. Svatos, A., Valterova, I., Saman, D., Vrkoc, J., (**1990**) *Chem. Commun.*, 55, 485.
131. Aguilar, J. A., Faulkner, S., Nilsson, M., Morris, G. A., (**2010**) *Angew. Chem. Int. Ed.*, 49, 3901.
132. Aguilar, J. A., Nilsson, M., Morris, G. A., (**2011**) *Angew. Chem. Int. Ed.*, 50, 9716.
133. Nilsson, M., Morris, G. A., (**2007**) *Chem. Commun.*, 933.
134. Morris, G. A., Aguilar, J. A., Evans, R., Haiber, S., Nilsson, M., (**2010**) *J. Am. Chem. Soc.*, 132, 12770.
135. Paudel, L., Adams, R. W., Király, P., Aguilar, J. A., Foroozandeh, M., Cliff, M. J., Nilsson, M., Sándor, P., Waltho, J. P., Morris, G. A., (2013) *Angew. Chem. Int. Ed.*, 125, 11830.

136. Adams, R.W., Byrne L., Király P., Foroozandeh M., Paudel L., Nilsson M., Clayden J., Morris, G. A., (**2014**) *Chem. Comm.,* 50, 2512.
137. Aquilar, J. A., Morris, G. A., Kenwright, A. M., (2014) *RSC Adv.,*4, 8278.
138. Zangger, K., Sterk, H., (1997) *J. Magn. Reson.,* 124, 486.
139. Aguilar, J. A., Faulkner, S., Nilsson, M., Morris, G. A., (2010) *Angew. Chem., Int. Ed*., 49, 3901.
140. Giraud, N., Béguin, L., Courtieu, J., Merlet, D., (2010) *Angew. Chem., Int. Ed*., 49, 3481.
141. Meyer, N. H., Zangger, K. (2013) *Angew. Chem., Int. Ed.,* 52, 7143.
142. Byrne, L., Sola` J., Boddaert, T., Marcelli, T., Adams, R. W., Morris, G. A., Clayden, J., (2014) *Angew. Chem., Int. Ed*., 126, 155.
143. Castañar, L., Nolis, P., Virgili, A., Parella, T., (2013) *Chem. Eur. J*., 19, 17283.
144. Ying, J., Roche, J., Bax, A., (2014) *J. Magn. Reson*., 241, 97.
145. Paudel, L., Adams, R. W., Király, P., Aguilar, J. A., Foroozandeh, M., Cliff, M. J., Nilsson, M., Sándor, P., Waltho, J. P., Morris, G. A., (2013) *Angew. Chem., Int. Ed*., 52, 11616.
146. Castañar L., Pérez-Trujillo, M., Nolis, P., Monteagudo, E., Virgili, A., Parella, T., (2014) *ChemPhysChem*, 15, 854.

Sachin Rama Chaudhari, was born on August 17th, 1986, and obtained his B.Sc. Degree in 2006 from the Sardar Patel Mahavidyalaya, Chandrapur affiliated to Nagpur University, Maharashtra. He completed his M.Sc. (Physical Chemistry) Degree in 2008 from Nagpur University, Maharashtra. He joined the Solid State and Structural Chemistry Unit and NMR Research Centre, Indian Institute of Science, Bangalore, for the Ph.D. program in August 2009. He qualified in the CSIR-UGC joint National Eligibility Test (NET) in June 2009, SET Exam (Maharashtra state) January-2009 and is presently a Research Associate in the department. The author's primary research interests are in NMR spectroscopy; with special interest on application to small molecules and its methodological development. He was awarded for Excellence research in India in the field of NMR spectroscopy for the year-2012 and selected for the Jharana Rani Samal Best Student Award for the year 2013 by the National Magnetic Resonance Society, India.

N. Suryaprakash, Ph.D. 1986, Bangalore University, Bangalore, Postdoctoral research at University of Basel, Switzerland, 1990–91 (Prof. Peter Diehl), Ben Gurion University of the Negev, Israel; 1998–1999 (Prof. Raz Jelinek) University of Southampton, United Kingdom 1999–2000 (Prof. J.W. Emsley). Presently Professor at NMR Research Centre, Indian Institute of Science, Bangalore. Elected Fellow of National Academy of Sciences, Allahabad, India (2005). **Research Interests:** Development of multi dimensional single quantum and multiple quantum NMR Methodologies. Structures of molecules in the liquid crystalline media, NMR Methods for the study of enantiomers, weak molecular interactions.